UNIVERSIDADE DE SÃO PAULO
INSTITUTO DE GEOCIÊNCIAS

Comparison of temperature of metamorphism using quartz c-axis fabric thermometer, Zr-in-rutile and Ti-in-quartz, using as example quartzite samples of the Carrancas Group, MG, Brazil

BEATRIZ PONTES ARAÚJO

Dissertação apresentada ao Programa de Geociências (Mineralogia e Petrologia) para obtenção do título de Mestre em Ciências

Área de concentração: Petrologia Ígnea e Metamórfica

Orientador: Prof. Dr. Renato de Moraes

SÃO PAULO
2018

Serviço de Biblioteca e Documentação do IGc/USP
Ficha catalográfica gerada automaticamente com dados fornecidos pelo(a) autor(a)
via programa desenvolvido pela Seção Técnica de Informática do ICMC/USP

Bibliotecários responsáveis pela estrutura de catalogação da publicação:
Sonia Regina Yole Guerra - CRB-8/4208 | Anderson de Santana - CRB-8/6658

Pontes Araújo, Beatriz Comparison of temperature of metamorphism using quartz c-axis fabric thermometer, Zr-in-rutile and Ti-in-quartz, using as example quartzite samples of the Carrancas Group, MG, Brazil / Beatriz Pontes Araújo; orientador Renato de Moraes. -- São Paulo, 2018.
53 p.

Dissertação (Mestrado - Programa de Pós-Graduação em Mineralogia e Petrologia) -- Instituto de Geociências, Universidade de São Paulo, 2018.

1. Grupo Carrancas. 2. Platina Universal. 3. EBSD. 4. Ti-em-quartzo. 5. Zr-em-rutilo. I. de Moraes, Renato, orient. II. Título.

AGRADECIMENTOS

Gostaria de agradecer ao meu orientar Prof. Dr. Renato pela parceria e paciência por ter me guiado nestes últimos quatro anos de trabalho, foi um grande aprendizado. Ao Professor Dr. Frederico Faleiros que me ajudou bastante desde o trabalho de formatura.

Aos laboratórios do Instituto de Geociências da USP que apoiaram nas análises deste trabalho e aos especialistas: Marcos e Leandro do Laboratório de Microssonda Eletrônica e Vinícius do Laboratório de Química e ICP. E ao laboratório LAME-LACTEC da Universidade Federal do Paraná, sob coordenação do Professor Dr. Leonardo Lagoeiro.

Agradeço à minha família: meus pais, Elisabeth e Valdir, meus irmãos, Fernando e Fabio, e irmã, Bruna, pelo carinho e acolhimento quando eu precisei.

Ao Felipe, meu querido, que me acompanhou durante o trabalho nos momentos fáceis e difíceis, obrigada pela paciência, o conforto que você me proporciona não pode ser medido em palavras.

Aos meus amigos de longa data do colégio Bandeirantes, que até hoje brincam que eu trabalho com pedras, nossos caminhos foram diferentes, mas a amizade continua.

Aos alunos de graduação que fiz amizade, de todos esses oito anos no instituto, aos colegas e amigos da pós-graduação, dos diversos corredores nos quais estamos espalhados, sou muito agradecida pela companhia e conselhos durante os anos de pós-graduação.

Gostaria de agradecer ao projeto FAPESP (16/22627-3) pelo apoio financeiro deste trabalho e a CNPq pelo apoio financeiro.

ABSTRACT

Quartz is one of the most common minerals in the Earth's crust, and is an important constituent of many metamorphic rocks. Because of the correlation between the dynamic recrystallization mechanisms and temperature, it is possible to understand the relationship between deformation and metamorphism evolution with the investigation of quartz, its textures, crystallographic orientation and its trace elements composition.

Recently, thermometer calibrations were proposed based on the relationship between c-axis fabric open angle. Studies show that trace elements are also reliable indicators for geothermometers, especially on rocks without metamorphic index minerals,, such as in quartzites. With these calibrations it is possible to investigate the metamorphic-deformational evolution and compare to the metamorphic evolution of associated rocks containing diagnostic paragenesis and *P-T* conditions, allowing the full picture of establishment of the relationship between deformation and metamorphism.

The aim of this research is to evaluate the c-axis thermometer, using data from Universal Stage and Electron Backscatter Diffraction (EBSD), as well as trace elements thermometry, Ti-in-quartz and Zr-in-rutile. The study was conducted on quartzites of the Carrancas Group, on Serra da Estância, Serra do Pombeiro and Serra de Carrancas, which *P-T* conditions of metamorphism were established with great precision in previous works. The study area is located in the southern region of Minas Gerais, near the cities of Carrancas, Itutinga, Itumirim and Lavras.

Temperatures obtained by the c-axis thermometer were confronted with previously processed data and produced different results for each method, Universal Stage and EBSD. The Universal Stage produced a temperature that fits very well with metamorphic peak from previously calculated temperatures, and it seems to be a very reliable, cheap and relatively fast method.

The stereograms made with EBSD data produced blurred girdles. It is not clear if the acquired data was either made properly or if this is a result of superimposed events of deformations, as suggested by petrography.

The Zr-in-rutile thermometer partially agrees with the thermobarometry results of the literature, because at temperatures below 600 °C, it does not activate the zircon to participate on cation exchange reactions with other minerals, so the Zr concentration on rutile is considered to be from the source rock, and not related to deformation or metamorphism.

The Ti-in-quartz was not a reliable thermometer for this case study. The temperatures are higher than the expected and the hypothesis is that the quartz grains might not have enough energy to exchange cations with rutile and zircon during the deformation and metamorphism caused by shear zones on Carrancas *klippe*. For further investigation, it is interesting to use cathodoluminescence that might map the Ti concentration zones on quartz grains to identify portions with different Ti concentrations and investigate their relationship with possible recrystallization textures.

KEYWORDS: Carrancas Group; Universal Stage; EBSD; Ti-in-quartz; Zr-in-rutile

RESUMO

O quartzo é um dos minerais mais comuns na crosta terrestre e é um constituinte importante de muitas rochas metamórficas. Devido à correlação entre os mecanismos dinâmicos de recristalização e a temperatura, é possível entender a relação entre a deformação e a evolução do metamorfismo com a investigação do quartzo, suas texturas, orientação cristalográfica e sua composição de elementos traços.

Recentemente, calibrações de termômetros foram propostas com base na relação entre o ângulo de abertura do eixo-c. Estudos mostram que elementos traços também são indicadores confiáveis para geotermômetros, especialmente em rochas sem índices de minerais metamórficos, como os quartzitos. Com estas calibrações é possível investigar a evolução metamórfico-deformacional e comparar com a evolução metamórfica de rochas associadas contendo paragênese diagnóstica e condições de P-T, permitindo o quadro completo do estabelecimento da relação entre deformação e metamorfismo.

O objetivo desta pesquisa é avaliar os termômetros de eixo-c, utilizando dados de Platina Universal e de *Electron Backscatter Diffraction* (EBSD), e temperatura de elementos traço, Ti-em-quartzo e Zr-em-rutilo. O estudo foi realizado nos quartzitos do Grupo Carrancas, na Serra da Estância, Serra do Pombeiro e Serra de Carrancas, cujas condições de metamorfismo da *P-T* foram estabelecidas com grande precisão em trabalhos anteriores. A área de estudo está localizada na região sul de Minas Gerais, próximo às cidades de Carrancas, Itutinga, Itumirim e Lavras.

As temperaturas obtidas pelo termômetro do eixo c foram confrontadas com dados previamente processados e produziram resultados diferentes para cada método de Platina Universal e EBSD. Os dados de platina produziram temperaturas que se encaixam muito bem com o pico metamórfico de temperaturas previamente calculadas, e parece ser um método muito confiável, barato e relativamente rápido.

Os estereogramas feitos com os dados do EBSD produziram guirlandas pouco nítidas. Não está claro se os dados adquiridos foram feitos adequadamente ou se isso é resultado de eventos sobrepostos de deformações, como sugerido pela petrografia.

O termômetro de Zr-em-rutilo concordam parcialmente com os resultados de termobarometria da literatura, porque em temperaturas abaixo de 600 ° C, os minerais de zircão não são ativados para participar de reações de troca de cátions com outros minerais, portanto a concentração de Zr no rutilo é considerada como sendo da rocha fonte, e não relacionadas à deformação ou metamorfismo.

O Ti-em-quartzo não foi um termômetro confiável para este estudo de caso. As temperaturas são superiores às esperadas e a hipótese é de que os grãos de quartzo podem não ter energia suficiente para trocar cátions com rutilo e zircão durante a deformação e metamorfismo causados por zonas de cisalhamento na klippe Carrancas. Para investigações posteriores, é interessante utilizar catodoluminescência para que seja possível mapear as zonas de concentração de Ti em grãos de quartzo e assim identificar porções com diferentes concentrações de Ti e investigar sua relação com possíveis texturas de recristalização.

PALAVRAS-CHAVE: Grupo Carrancas; Platina Universal; EBSD; Ti-em-quartzo; Zr-em-rutilo

LIST OF FIGURES

LIST OF TABLES

SUMMARY

CHAPTER 1 - INTRODUCTION

Quartz is an important constituent of the rocks that comprise the continental crust, partially controlling its deformation behavior, taking part in several metamorphic reactions and allowing a connection between temperature and recrystallization microstructure (Kruhl, 1986; Stip, 2002; Law, 2014). Any research trying to link quartz deformation and temperature might shed light over the metamorphic-deformational evolution of metamorphic belts, helping to understand thermal evolution, variations in deformation mechanisms throughout its history and the processes involved in rock burial, metamorphism and exhumation.

The combination of recrystallization of quartz and its temperature of deformation led to a new branch of metamorphism study which still intrigues researchers. The study of the correlation of quartz c-axis plunge and temperature contributed to understanding the dynamic recrystallization of quartz-rich rocks (Kruhl, 1986; Stipp, 2002; Law, 2014). Hence, there are new calibrations (Faleiros *et al*., 2016) based on the first works of quartz c-axis that points out to more reliable deformation temperatures.

Several studies show that trace elements are reliable indicators for geothermometers, especially on rocks without minerals indexes (e.g. Zack *et al.*, 2004; Cherniak *et al.*, 2006; Wark and Watson, 2006; Tomkins *et al.*, 2007; Thomas *et al.*, 2010), such as quartzites. Besides the dynamic recrystallization for temperature and pressure estimation, the trace elements concentration is studied because of their direct influence on temperature of crystallization on rocks. Hence, the quartzite is a suitable rock, for its abundance on continental crust, for these analyses for studying metamorphism, once the Si is traded for Ti and Zr, in the lattice, on presence of rutile and zircon on the rock composition.

The Carrancas group is dominated by quartzite on its stratigraphy, and because of the variation of metamorphism grade along the region, quartzite is a convenient rock for this study of quartz c-axis tilt and trace elements thermometer for understanding the metamorphism grade on the study area.

1.1 Geological Setting

The investigated rocks are from the Carrancas Group (Trouw *et al*., 1983), part of the Carrancas Nappe System, in the Southernmost Brasília Orogen (Campos Neto *et al*., 2004), which defines the southwestern boundary of the São Francisco Craton (Figure 1). The Carrancas Nappe System consists of a group of four thrust sheets: Luminárias Nappe,

Carrancas Klippe, Serra da Bandeira Allocthonous and Madre de Deus Allocthonous (Campos Neto *et al*., 2004, 2011).

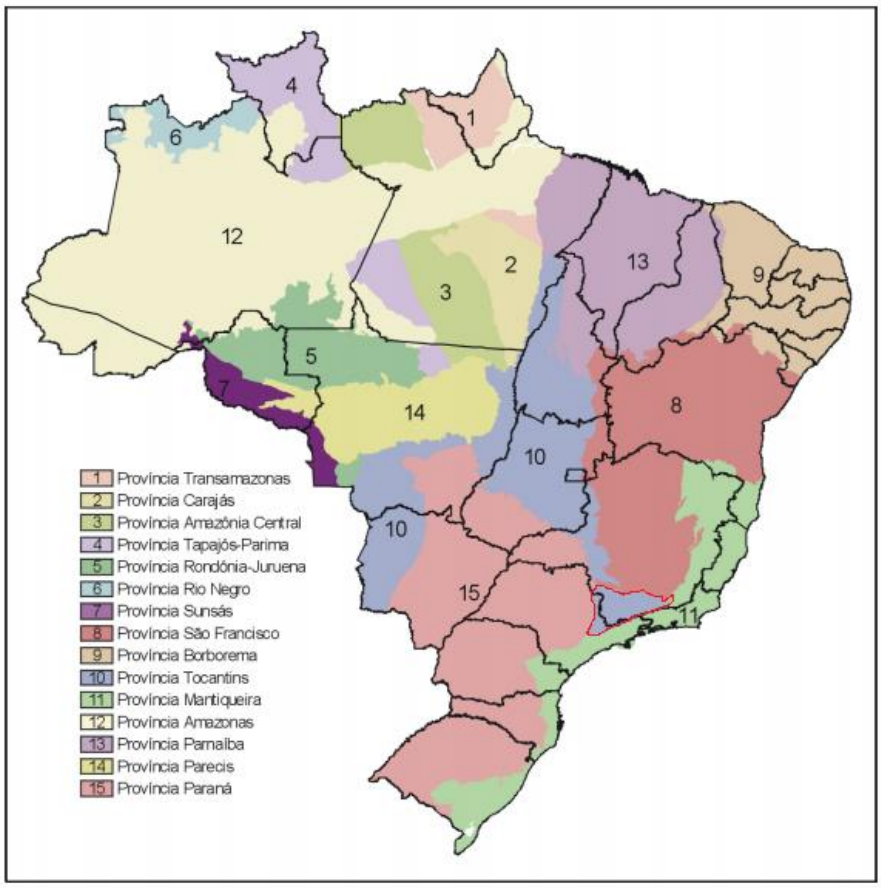

Figure 1: The main Structural Provinces of Brazil, with the Southern Brasília Orogen in red (Modified from Bizzi *et al*., 2003).

The Southernmost Brasília Orogen is divided in two main different tectonic domains, rocks related to the active margin and passive margins. The domains associated with the active margin are, from top to bottom, the Socorro-Guaxupé Nappe, a magmatic arc domain developed on the active continental margin (Campos Neto, 2000) and Andrelândia Nappe System, a sedimentary domain of subducted continental crust (Figure 2; Campos Neto *et al*., 2004). The domains associated with the passive margin are related to the São Francisco Craton itself and older metasedimentary rocks deformed during the Neoproterozoic, such as the São Vicente Complex (Paciullo *et al*., 1996), renamed as A1 and A2 units of Paciullo *et al*. (2000), which were taken as the authoctonous portion of the Andrelândia Megasequence (Ribeiro et al., 1995) and later it was discovered it was deposited during the Paleoproterozoic

(Westion & Campos Neto, 2013; Figure 4), as well as the rocks of the Carrancas and Lima Duarte Nappes (Campos Neto, 2000).

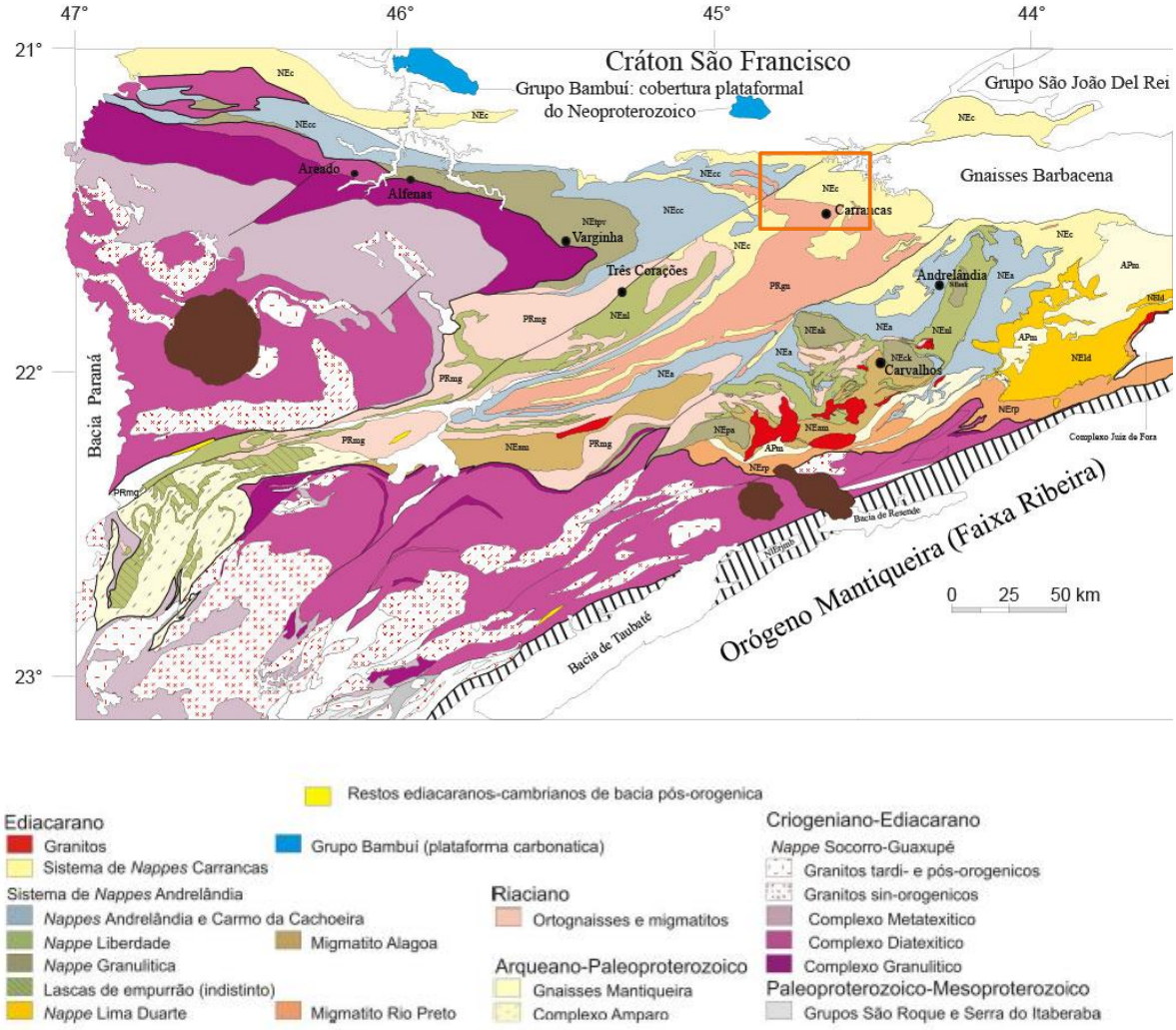

Figure 2: Simplified geological map of the Southern Brasília Orogen (according to Campos Neto et al., 2011), in which the box highlight the study area.

1.1.1 The Carrancas Group

The Carrancas Group was defined by Trouw *et al.* (1983) and it crops out in the homonimous and surrounding hills, Serra do Pombeiro, Serra da Estância and Serra de Carrancas (Figure 3). Ribeiro and Heilbron (1982) divided the metasedimentary units of Carrancas Group into two different sets: allochthonous and autochthonous, where autochthonous set was named São João del Rei Group, on the bottom, and made of biotite schist and a graphitic phyllite with few quartzite lenses; at its top there are biotite schist, biotite-chlorite phyllite and biotite gneiss, with centimetric quartz venules (Ribeiro and

Heilbron, 1982). The allochthonous unit is what is though as the real Carrancas Group, and composed of a sequence of quartzite and schist, which occurs in the Serras do Pombeiro, Carrancas and Estância, and is in tectonic contact to the biotite schist and graphitic schist of the autochthonous unit (Heilbron, 1983).

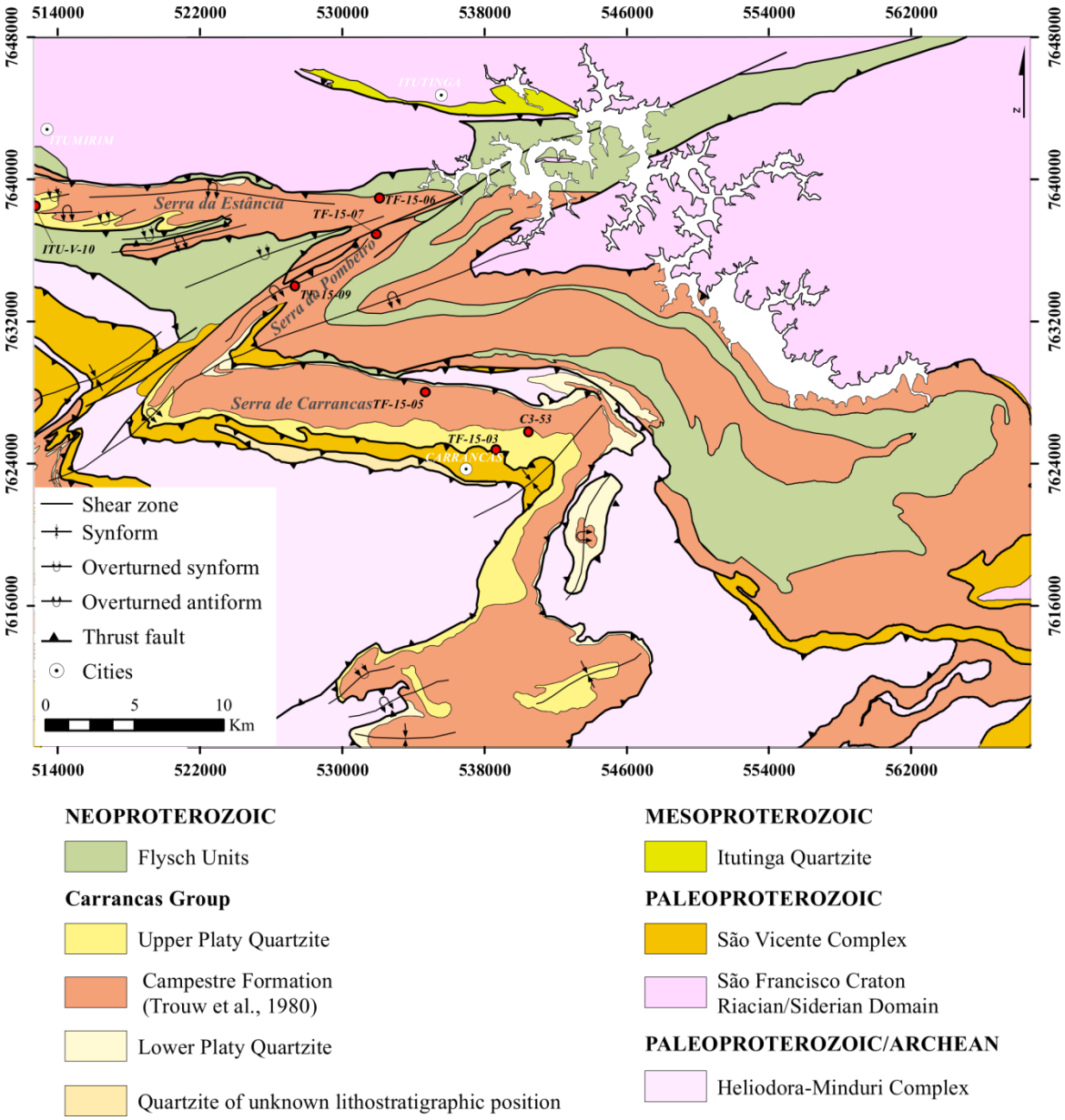

Figure 3: Geological map of the Carrancas region, with the samples locations, including Serra da Estância, Serra de Carrancas and Serra do Pombeiro. Modified from Paciullo et al. (2002), Ribeiro et al. (2002) and Westin (2015).

The Carrancas Group was originally divided into two formations, from the base to the top, the São Tomé das Letras and Campestre Formations (Ribeiro & Heilbron, 1982), after that, the Chapada das Perdizes Formation was added to the top (Coutinho, 2012). The São

Tomé das Letras Formation is composed of a quartzite muscovite sequence, with green mica, with black tourmaline and opaque minerals as the main accessories, which transition to muscovite-quartz schist and muscovite schist. The Campestre Formation consists of intercalations of phyllite or schist, with or withouth graphite, and quartzite with white mica (Ribeiro & Heilbron, 1982; Trouw *et al*., 1983). From North to South, the phyllite is replaced by schist (Silva, 2010). The Chapada das Perdizes is lithological identical to the São Tomé das Letras, but it sits on the top of the Carrancas Group (Coutinho, 2012).

1.1.2 Depositional History

The Southern Brasília Orogen has been studied for many years and many authors have theorized about its depositional settings and origins (Ebert, 1968, 1971; Trouw *et al.*, 1989; Ribeiro *et al.*, 1995; Paciullo *et al*., 2000; Campos Neto *et al*., 2004, 2011).

The original idea is that the origin and depositional settings of sediments of Andrelândia, São João del Rei and Carrancas Groups may have belonged to the same tectonic-sedimentary cycle (Ebert 1968, 1971; Trouw *et al.*, 1983, 1989). However, Ribeiro *et al*. (1995) recognized four depositional cycles, namely, Tiradentes (quartzite) Lenheiro (quartzite), Carandaí (pelites and limestone) and Andrelândia (metarenites and pelites) in stratigraphic order. Based on these cycles, the authors defined three Proterozoic depositional basins, São João del Rei, Carandaí and Andrelândia, the first two intracontinental and the last one of passive continental margin.

The Andrelândia and Carrancas groups were grouped into the Andrelândia Megasequence, divided into six units (Paciullo *et al*., 2000): A1 - paragneiss; A2 - paragneiss, quartzite and schist; A3 - quartzite; A4 - gray phyllite / schist; A5 - biotite schist / gneiss; A6 - schist and paragneiss, minor quartzite, metachert and calc-silicate rocks (Figure 4). Due to a discontinuity, units A1 is considered the authoctonous portion, A1 to A4 correspond to the Carrancas Sequence, allochthonous domain, whereas the A5 and A6 units to the Turvo Sequence, also corresponds to the allochthonous domain (Figure 4).

Campos Neto *et al.* (2011) considered that the Andrelândia Megasequence is, in fact, a set of nappe systems with different ages of metamorphism, having between 620 Ma and 595 Ma (Campos Neto, *et al.*, 2011), and Carrancas Nappe System, with a outward motion dating at 590 Ma (Campos Neto, *et al*., 2011).

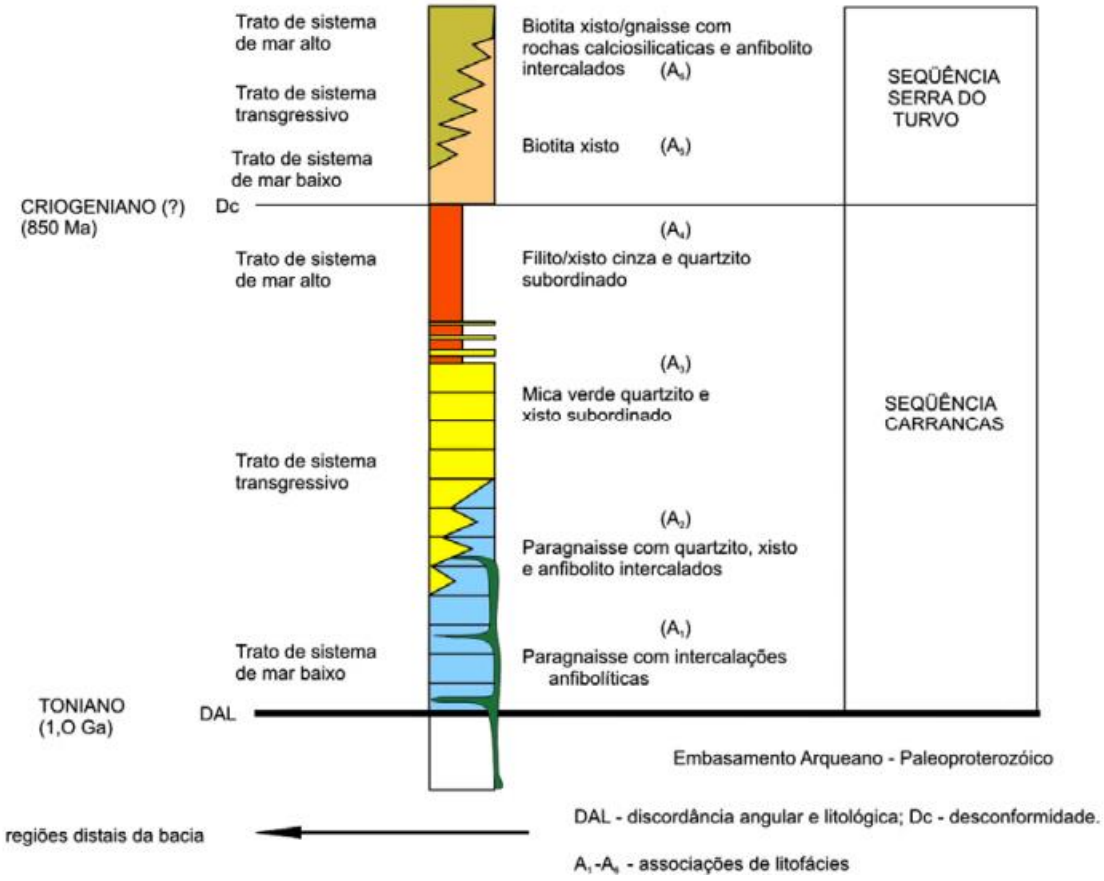

Figure 4: Stratigraphy of Andrelândia Megasequence. Extracted from Ribeiro *et al.* (2003).

The São Vicente Complex was defined by Paciullo *et al*. (1996, 2000) as units A1 and A2, it has depositional ages of 2170 My, 2140 My and 2130 My, obtained by U-Pb, Lu-Hf and Sm-Nd methods (Westin & Campos Neto, 2013; Westin *et al.*, 2016). Thus, the rocks of the São Vicente Complex are older than those of the Andrelândia Nappe System and Carrancas Group, and the maximum age for deposition of the metapelites with quartz lobes of the Campestre Formation of the Carrancas Group, based on the youngest modal class, is within the Tonian period (Westin & Campos Neto, 2013).

1.1.3 Structural Geology

At least three phases of deformation are recognized in Carrancas Group (Trouw *et al.*, 1983; Heilbron, 1983). D1 was responsible for the formation of regional and penetrative slate cleavage, represented by the parallelism of metamorphic micas (Heilbron, 1983), few folds and large push movements that distributed the rocks in scales and nappes. The deformation phase D2 is represented by folds with sub-horizontal axial surface (S2) and axes approximately EW (E2), which were refolded by D3, responsible for the formation of open or

tight folds, millimeter-to-kilometric scale, pronounced dips in axial planes for SE-E, 0 to 35 °, (Heilbron, 1983), usually for SE or optionally NW (Trouw *et al*., 1983). A fourth phase of deformation (D4) was originated at shallower crustal levels, and produced folds and crenulation of D2 and D3. The D4 folds have axes with direction for NE-SW and N-S, with S and SW plunge, steep axial planes and vergence for NW. This deformation is responsible for the formation of the mega structure in "M" or "Z" in the E-W direction of Serra de Carrancas (Figure 3; Coutinho, 2012).

1.1.4 Metamosphism

The metamorphism of the studied region was characterized as a barrovian type, with the presence of almandine, kyanite, staurolite and sillimanite, with increasing temperature from north to south, reaching its climax during the second phase of deformation (Trouw *et al*., 1983). In the region of the Serra do Pombeiro and Serra de Carrancas it was possible to map three metamorphic isograds, ranging from the green schist to the upper amphibolite facies: garnet-in, staurolite-in and chloritoid-out. As the metamorphic isograds are oblique to the direction of the layers and pass straight from the allochthonous to the autochthonous rocks, they are later than the first phase of deformation, which were responsible for the tectonic stacking of the allochthonous facies on the autochthonous (Ribeiro & Heilbron, 1982).

Therefore, the rocks of Carrancas Nappe System, located in the northern region, are characterized by biotite- or chloritoid-bearing green schists facies assemblage (Ribeiro *et al*., 1995; Campos Neto & Caby, 2000), whereas in the southern portion, the mineral assemblage bears garnet, staurolite and, sometimes, the pair biotite-kyanite always lacking chloritoid, which points out to a amphibolite facies conditions (Ribeiro *et al*., 1995).

Pseudosections and thermobarometry demonstrated that the metamorphism is progressive from north to south (Figure 3), however the pressure regime is not barrovian but happened at higher pressure, in the transition between amphibolite and eclogite facies (Silva, 2010). Metamorphic peak conditions of 586 ± 2 °C and 10.65 ± 0.65 kbar were determined for the rocks of the Serra da Estância, with paragenesis of chloritoid, chorite, staurolite, muscovite and quartz, while for the rocks of Serra de Carrancas, the metamorphic peak was reached at 620 ± 5 ° C and 12.2 ± 0.5 kbar, with the paragenesis of quartz, muscovite, garnet, staurolite and kyanite (Pavan, 2010). Further south, in Serra das Bicas, the paragenesis is made up of quartz, muscovite, garnet, biotite and kyanite, without staurolite that yielded metamorphic peak conditions of 641 ± 35 ° C and 11.16 ± 2.2 kbar (Garcia, 2010).

1.2 Research Aims

The aim of this research is to use the c-axis quartz thermometer to investigate variations of metamorphism in an area where metamorphic conditions is know, as in the Carrancas region, to check how precise the thermometer can reproduce the conditions of peak of metamorphism or later stages of deformation.

1.3 Material and methods

Seven oriented quartzite samples were collected for the study of quartz microstructures, in universal stage, electron backscattered diffraction (EBSD). The same samples are used for the analyses of Ti-in-quartz and Zr-in-rutile thermometers. All thin sections were made with cuts parallel to stretching lineation and perpendicular to foliation.

1.3.1 Quartz Dynamic Recrystallization

Quartz is a very abundant mineral in the Earth's crust, and knowledge about its mechanisms of deformation has increased considerably in recent decades (eg White, 1977; Kruhl, 1986; Passchier & Trouw, 2005; Derez *et al*., 2015). According to Passchier & Trouw (2005) there are four types of factors that influence quartz deformation: temperature, water pressure, strain rate and differential stress. The temperature imparts great influence and controls different types of deformation in the crystalline lattice. The water pressure favors the increase of the rates of recrystallization and granular growth. The strain rate and the differential stress are related to the different pressures that act on the modification of the crystalline reticular geometry.

Recrystallization is the reorganization of material with the change of size, shape and orientation of the mineral (Passchier & Trouw, 2005). Quartz exhibits different behavior over recrystallization at different temperature ranges and can be separated into three different types: bulging, subgrain rotation recrystallization and grain boundary migration (Figure 5; Stipp *et al*. 2002). Bulging occurs at temperatures between 250 and 350 ºC, where the mineral grain boundary undergoes displacements that diminish its size and generate the formation of subgrains and smaller grains on its edges (Passchier & Trouw, 2005). These are formed due to the difference in displacement density between two quartz grains that are in contact and the subgrains are formed where there is greater displacement density (Passchier & Trouw, 2005). Subgrain rotation recrystallization occurs at temperatures between 350 and 450 ºC, and is

characterized by the gradual change of subgrains with low angle contacts for subgrains with high-angle contacts, forming new recrystallized grains when the degree of rotation of the crystalline lattice is higher than 5-10 ° (Passchier & Trouw, 2005). Grain boundary migration occurs at high temperatures, above 450 °C, when compared to the two previous mechanisms, where the mobility of the grain contact occurs, and a grain with a crystalline lattice stable in relation to the strain ends consuming parts or other whole grains, whose lattice presents unfavorable orientation (Passchier & Trouw, 2005). It is not uncommon in this mechanism to increase the mean grain size in the rock (Passchier & Trouw, 2005).

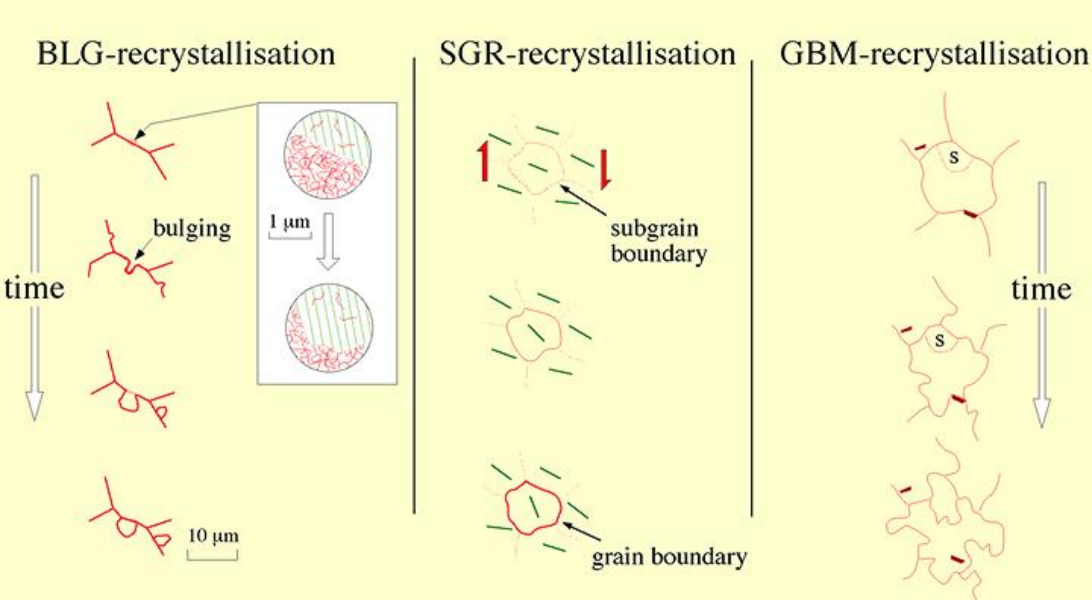

Figure 5: BLG - the edge of the mineral grain undergoes displacements that diminish its size and generate the formation of subgrains and smaller grains on its edges. These are formed due to the difference in displacement density between two quartz grains that are in contact and the subgrains are formed where there is greater displacement density. SGR - causes the formation of grain edges subgrains, this new grain is developed by the forward rotation of subgrains structure of a larger grain. GBM – occurs by the mobility of the contact of the grains, being a grain, with crystalline lattice in position more stable in relation to the efforts, ends up consuming parts or other whole grains, whose lattice presents unfavorable orientation and thus, increasing its border area (Passchier and Trouw, 2005).

There are several techniques to determine the temperature and pressure of quartz-rich rocks that were submitted to tectonic events, such as quartz-c-axis deformation or even recrystallization textures (Law, 2014). The work of Kruhl (1986) is one of the pioneers in the subject and it is based in the relationship between textures, mechanisms of deformation and temperature in which quartz crystals were deformed. The quartz crystals are trigonal, thus

having a prismatic axis of longer elongation, the <c>, and the basal, of smaller elongation, the <a> (Kruhl, 1986). By deformation of the first, it is possible to determine the rate of deformation, in which the rock was conditioned and, consequently, to have an idea of the temperature, since different mechanisms of deformation act at different temperatures (Kruhl, 1986). Recrystallization of quartz crystals is the product of the relationship of high stresses on rocks and temperature (Kruhl, 1986). Thus, the higher the deformation rate, the higher the deformation of the quartz. It has been identified that the basal axis, <a>, is affected primarily at low temperatures and stresses, whereas the c-axis at low temperatures and stresses (Kruhl, 1986). A first, semi-quantitative, quartz-c-axis thermometer was based on the quartz crystal recrystallization texture, and the influence of strain rates and c-axis response was already recognized (Kruhl, 1986).

1.3.2 Quartz c-axis thermometer

The orientation of quartz c-axis can be measure in a thin section using a regular optical microscope with a coupled universal stage and then all measures can be plot in a regular stereogram. The disposition of c-axis characteristic patterns and figures in stereograms and the angle between their maximum concentrations is called opening angle (Figure 6). Once it was established a relationship between the opening angle of the arrangement and distribution of quartz c-axis in stereogram and temperature, Law (2014) proposed an empirical calibration of the quartz c-axis thermometer. The thermometer is based on the correlation between temperature and quartz deformation mechanisms, which influence the degree of orientation of the mineral c-axis. This is evaluated by the opening angle (OA) of the figure formed in stereogram when the c-axis orientation is plotted, which is measured in thin sections cut parallel to the lineation and perpendicular to foliation. The thermometer was calibrated empirically through literature compiled data, for which calculated temperature conditions were determined for rocks that present study of c-axis orientation in quartz (Figure 6). It is considered that the thermometer produces good results between 300 and 650 °C (Law, 2014). Temperature derived from opening angle may be subjected to more than one interpretation, as during rock deformation, not only temperature and pressure are acting as intensive variables, but also, factors such as the presence of aqueous fluids and late superimposed deformation. The presence of water can produce weakening of quartz crystals, increasing the tension between them, and thus increasing the rate of recrystallization and grain growth. Late deformation can affect the interpretation or interfere with opening angle, leading

to erroneous results and a careful comparison between opening angle, temperature and observed quartz recrystallization microstructures must take into account, before interpretations are made (Law, 2014).

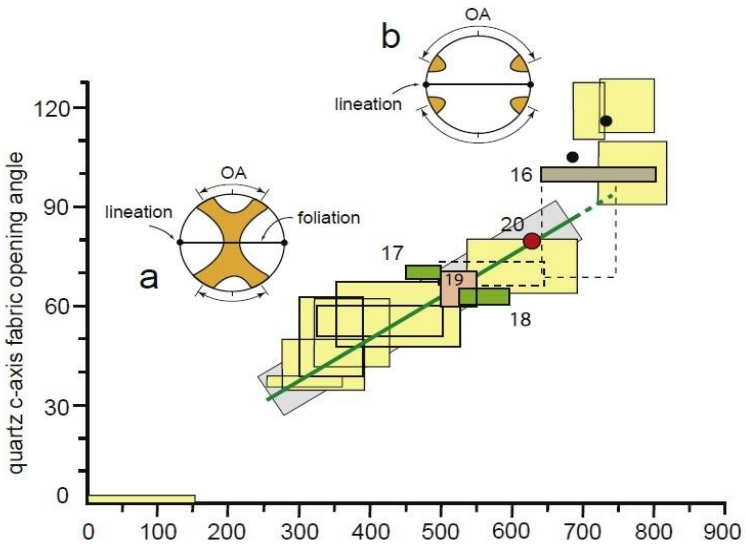

Figure 6: Modified plot of quartz c-axis fabric opening-angle versus deformation temperatures from naturally deformed rocks by Morgan and Law (2004). The squares represent results of samples studied in Morgan & Law (2004). The Green line represents the direct relation of temperature and quartz c-axis opening angle (after Law 2014). (a) and (b) are two schematic examples of crossed-girdle.

Faleiros *et al.*, (2016) established a new empirical calibration (1) for quartz c-axis fabrics that underwent deformation with temperatures above 650 °C and, further the temperature and opening angle (OA) dependencies, the influence of pressure on this thermometer was considered. With this new calibration, a new OA thermometer was compiled with temperatures ranging from ~250 to ~1050 °C and pressures around ~2.5 to ~15 kbar (Figure 7; Faleiros *et al.*, 2016).

$$T(°C) = 410.44 \times \ln AO + 14.22\, P\ (\text{kbar}) - 1272 \quad (1)$$

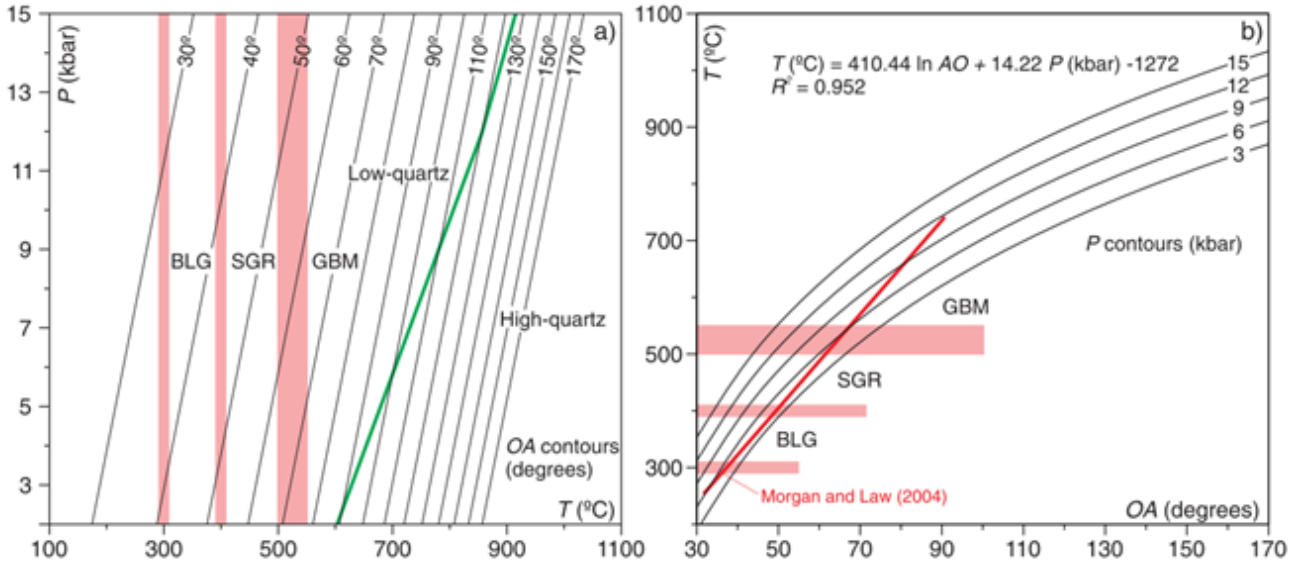

Figure 7: Contours of opening-angle in the *P–T* field (a) and of pressure in the *T*– OA field; the green line shows the transition between low- to high- quartz (b) calculated using the new OA thermometer; the boundaries of dynamic recrystallization of quartz is shown in the red boxes on both *P-T* and OA-*T* fields (modified from Faleiros *et al.*, 2016). The red line on (b) is the calibration made by Morgan & Law (2004) that Faleiros *et al*. (2016) verified with the new calibration.

1.3.3 Universal Stage

The universal stage is designed for any instrument that can be adjusted to the stage of an optical microscope in order to allow the rotation of a crystal around one or more axes in addition to the axis of the microscope itself (Figure 8). Thus, universal stage is used to the measurement of optical axis of minerals in rocks, allowing the statistical analysis of these in equal areas stereographic networks (Wahlstrom, 1969).

Figure 8: Leitz Wetzlar petrographic microscope with a coupled universal stage.

Universal stage is used to determine the angle required for the c-axis of a grain to be horizontal or vertical to obtain the plunge angle, hence the orientation of the axis relative to the foliation of the rock. For the determination of orientation of the quartz c - axis it was used a microscope with coupled universal stage. It has four to five axes that allow rotation of the thin section. The axes are referred to as east-west (A4), north-south (A2), internal vertical (A1), outer (A3) and the axis of the microscope stage (A5). In the rest positions, A1, A3 and A5 are parallel to the tube of the microscope and A2 and A4 are perpendicular to each other and are positioned in a horizontal plane. The thin section is located between glass hemispheres. The universal stage consists of different pairs of glass hemispheres of different refractive indexes, so depending on the mineral, indexes with values close to this one are used, avoiding the correction of angles due to possible differences between the indices of the glass hemisphere and of the mineral (Wahlstrom, 1969).

The thin section is placed on the glass disk, located in the middle of the attachment, which is attached to the horizontal axis of the stage. After centralizing a grain in the microscope, the chosen grains in axes A1, A2 and A3 are rotated, followed by extinctions and maximum illumination until the inclination of the c-axes of the grains measured is obtained (Figure 9). For each thin section, at least 300 quartz c-axis orientations were measured on a petrographic microscope Leitz Wetzlar, with a coupled universal stage, and these grains were measured along their exposure in the quadrant observed in the microscope, for the purpose of a more accurate statistic.

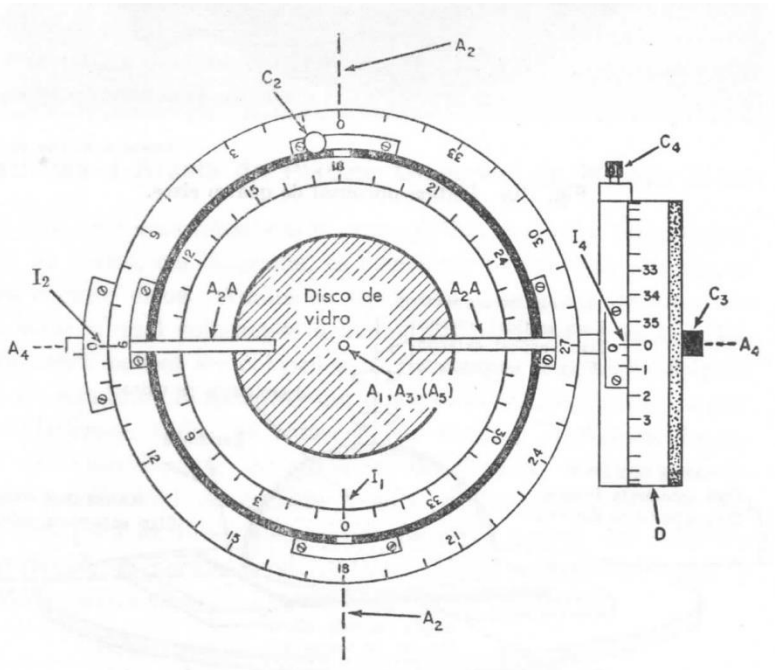

Figure 9: Scheme of the universal stage coupled to optical microscopes. A1, A2, A3 and A4 are the axes of rotation of the platinum and A5 is the axis of the microscope stage. C2, C3 and C4 are the screws that lock the axes A2, A3 and A4. A2A indicates the graduated vertical arcs for the A2 axis. I1, I2 and I4 are the indexes for the graduated circles for axes A1, A2 and A4. D is the graduated drum for rotating the stage around A4 (Wahlstrom, 1969).

1.3.4 Thermometers based on trace elements

Several studies show that trace elements are reliable indicators for geothermometers, especially on rocks without minerals indexes (e.g. Zack *et al.*, 2004; Cherniak *et al.*, 2006; Wark and Watson, 2006; Tomkins *et al.*, 2007; Thomas *et al.*, 2010). Besides the dynamic recrystallization for temperature and pressure estimation, the trace elements concentration is studied because of their direct influence on temperature of crystallization on rocks.

Ti has the same charge and similar ionic radius as Si, thus is able to replace Si on quartz tetrahedral sites conforming the influence of pressure and temperature. Wark and Watson (2006) developed the geothermometer "TitaniQ" (equation 2), which was set for pressures of 10 kbar, whereas the calibration made by Thomas *et al.* (2010), the pressures range from 5 to 20 kbar, thus the latter is more robust (equation 3). However, for the best results the TiO_2 activity (α_{TiO2}) in the rock must be ~ 1, which is assumed to be true in rutile-bearing rocks.

$$T(°C) = \frac{-3765}{\log\left(X_{Ti}^{qtz}\right) - 5.69} - 273 \quad (2)$$

$$T\ (°C) = \frac{a + cP}{b - R \times \ln X_{TiO_2}^{Qtz} + R \times \ln a_{TiO_2}} - 273.15 \quad (3)$$

The solubility of Zr-in-rutile was empirically studied by Zack *et al.* (2004), who identified its temperature dependency. However, Tomkins *et al.* (2007) with a set of experiments identified also a pressure dependency on Zr-in-rutile. The concentration of Zr increases along with the temperature, replacing the Ti on rutile structure, however, increasing the pressure, the concentration of Zr decreases (Figure 10). On Zack *et al*. (2004) the thermometer was relevant on the field of UHT metamorphism conditions and did not consider the pressure on *P-T* rocks conditions (equation 4).

$$T(°C) = 134.7 \times \ln(Zr\ in\ ppm) - 25 \quad (4)$$

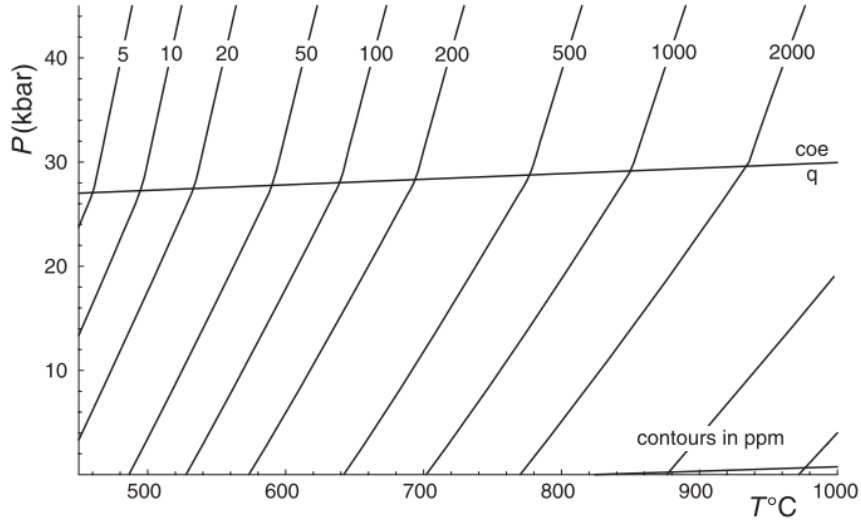

Figure 10: Thermometer as a *P-T* diagram for Zr-in-rutile, for the equilibrium of rutile-zircon-quartz polymorph (Tomkins *et al*., 2007).

Thomas *et al.* (2010) also estimated a calibration for determine the pressure, a thermobarometer, with a *P-T* diagram with known minimum and maximum concentrations of Ti-in-quartz and Zr-in-rutile on the same sample (Figure 11).

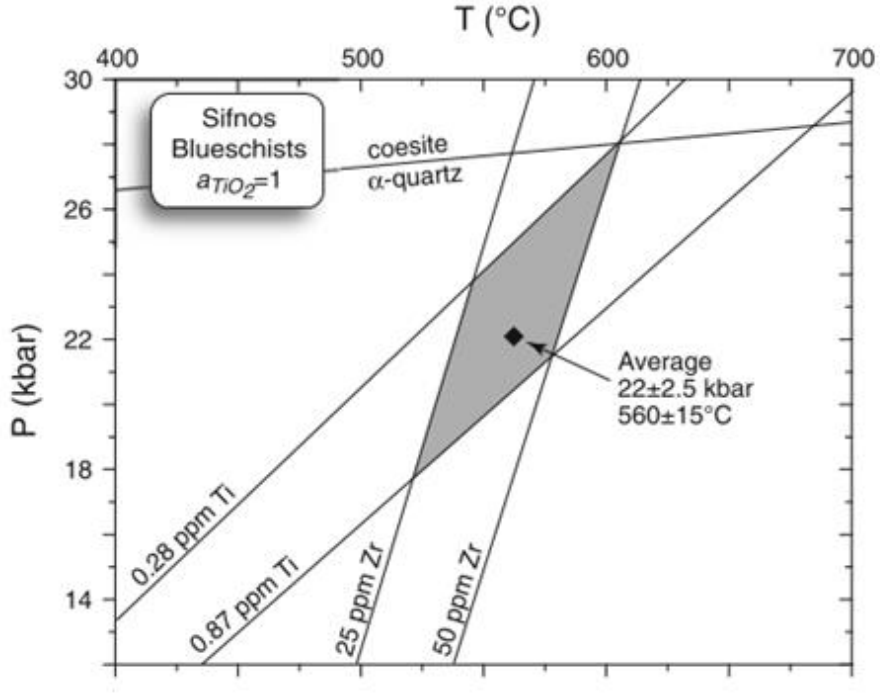

Figure 11: Application of concentrations in ppm of Ti-in-quartz and Zr-in-rutile solubility for usage as a thermobarometer to blueschists from Sifnos, Greece (Thomas *et al.*, 2010).

In this study, it was relevant to apply the Zr-in-rutile thermometer calculated by Tomkins *et al*., (2007), since the equation considers the pressure to get the corresponding temperature. The thermometer calculated by Tomkins *et al*., (2007) for α-quartz field is:

$$T(°C) = \frac{83.9+0.410P}{0.1428-R\ln\emptyset} - 273 \quad (5)$$

In which R is the gas constant, 0.0083144 kJ K^{-1}, and $\emptyset$ is the Zr concentration in ppm.

1.3.5 Electron Backscatter Diffraction

The Electron Backscatter Diffraction (EBSD) technique is used in a Scanning Electron Microscope (SEM) to map the crystallographic orientation and grains microstructures of many material sciences, as minerals, metals, semiconductor materials or even ceramics (Dingley *et al.*, 1995; Randle, 2000; Randle & Engler, 2000; Morales *et al.*, 2007). The EBSD is also used to phase identification and strain measurement (Randle, 2000). Combining the investigation of texture and microstructure, a more complete study of the sample is determined, permitting a better understanding of recrystallization, grain boundary structure, grain growth and many other orientation-dependent mechanisms (Goldstein *et al.*, 2007).

When the electron beam hits the tilted sample on the SEM stage, the electrons diffract following the Braggs law (6), forming a diffracted pattern, which is called Kikuchi pattern (Randle, 2000; Morales, 2007). Two cones per atom plane are observed because of the diffraction from the front and the back of the atomic planes (Goldstein, 2007). These two cones, when intercepted on the imaging plane (phosphor screen), are projected as two nearly straight lines separated by an angle of 2θ (Goldstein *et al.*, 2007).

$$\lambda = 2\mathrm{d}sen\theta \quad (6)$$

Where λ is the wavelength of the electrons, d is the spacing of the diffracting plane, and θ the angle of incidence of the electrons on the diffracting plane.

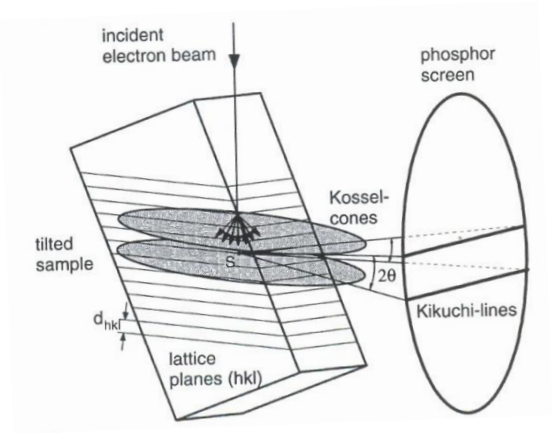

Figure 12: The diffracted electrons form the Kossel-cones which, as touching the phosphor screen, originate the Kikuchi lines (Randle and Engler, 2000).

As described in Randle (2000), the Kikuchi pattern is a set of lines where each pairs of lines, known as Kikuchi band, has a different width and matches a crystallographic plane. The lines are a result of the diffusely and inelastic behavior of the electron beam on the surface of the tilted sample (Figure 12). The intersections of the bands are called zone axes and correspond to specific crystallographic directions in the crystal (Goldstein *et al.*, 2007). The EBSD patterns are represented like a map of the angular intersections that each crystal has due to its crystallographic structure (Figure 13).

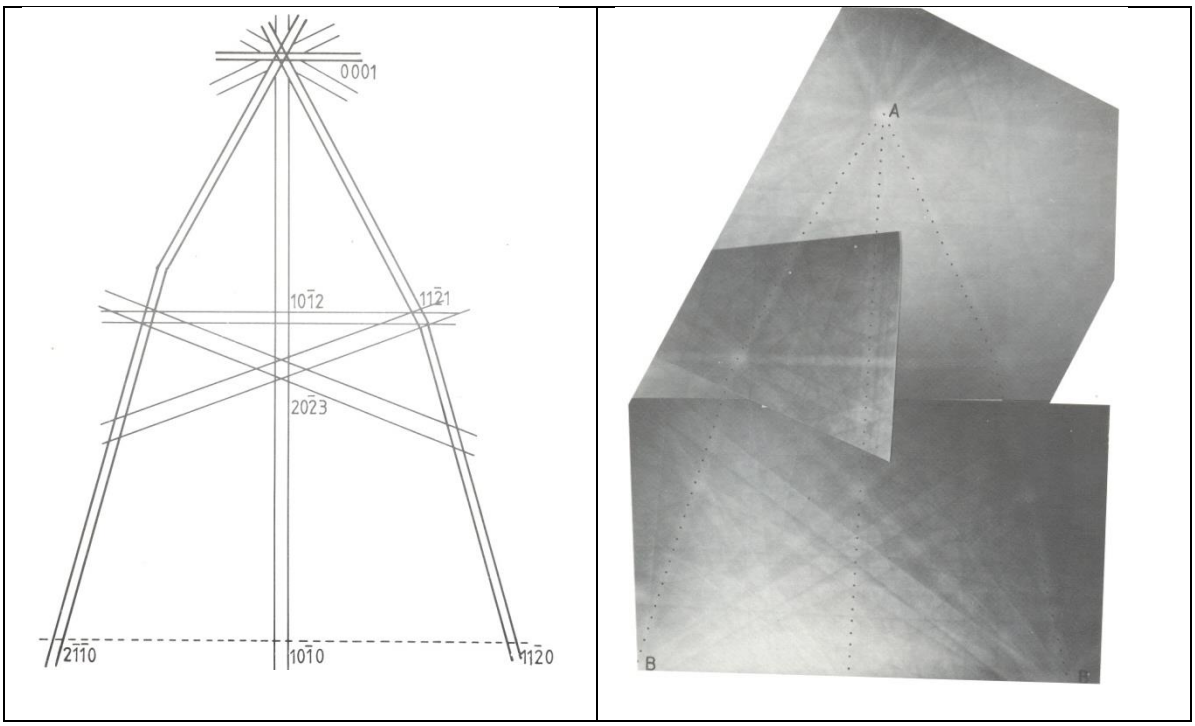

Figure 13: Quartz Kikuchi-pattern (Dingley *et al.*, 1995).

CHAPTER 2 - COMPARISON OF TEMPERATURE OF METAMORPHISM USING QUARTZ C-AXIS FABRIC THERMOMETER, ZR-IN-RUTILE AND TI-IN-QUARTZ, USING AS EXAMPLE QUARTZITE SAMPLES OF THE CARRANCAS GROUP, MG, BRAZIL

Araujo, B.P.; Moraes, R.; Faleiros, F.M.; Lagoeiro, L.

Abstract

Quartz is one of the most common minerals in the Earth's crust, and is an important constituent of many metamorphic rocks. Because of the correlation between the dynamic recrystallization mechanisms and temperature, it is possible to understand the relationship between deformation and metamorphism evolution with the investigation of quartz, its textures, crystallographic orientation and its trace elements composition.

Recently thermometer calibrations were proposed based on the relationship between c-axis fabric open angle and pressure. Studies show that trace elements are also reliable indicators for geothermometers, especially on rocks without minerals indexes, such as quartzites. With these calibrations it is possible to investigate the metamorphic-deformational evolution and compare with the metamorphic evolution of associated rocks containing diagnostic paragenesis and *P-T* conditions, allowing the full picture of establishment of the relationship between deformation and metamorphism.

The aim of this research is to evaluate the c-axis thermometer and trace elements by the methods of Universal Stage, Electron Backscatter Diffraction (EBSD), Ti-in-quartz and Zr-in-rutile, in quartz from units whose metamorphic evolution is known. Thus, the study was conducted on quartiztes of the Carrancas Group, on Serra da Estância, Serra do Pombeiro and Serra de Carrancas, which *P-T* conditions of metamorphism were established with great precision. The study area is located in the southern region of Minas Gerais, near the cities of Carrancas, Itutinga, Itumirim and Lavras.

Temperatures obtained by the c-axis thermometer were confronted with previously processed data and gave different results for each compared method, Universal Stage and EBSD. The Universal Stage produced a temperature that fits very well with metamorphic peak previously calculated, and it seems to be a very reliable, cheap and relatively fast method.

The stereograms made with EBSD data produced blurred girdles. It is not clear if the acquired data was either made properly or if this is a result of superimposed events of deformations, as suggested by petrography.

The Zr-in-rutile thermometer partially agrees with the thermobarometry results of the literature, because at temperatures below 600 °C, it does not activate the zircon to participate on cation exchange with other minerals, so the Zr concentration on rutile is considered to be from the source rock, and not related to deformation or metamorphism.

The Ti-in-quartz was not a reliable thermometer for this case study. The temperatures are higher than the expected and the hypothesis is that the quartz grains might not have enough energy to exchange cations with rutile and zircon during the deformation and metamorphism caused by shear zones on Carrancas *klippe*. For further investigation, it is interesting to use cathodoluminesence that might map the Ti concentration zones on quartz grains to identify portions with different Ti concentrations and investigate their relationship with possible recrystallization textures.

KEYWORDS: Carrancas Group; Universal Stage; EBSD; Ti-in-quartz; Zr-in-rutile

2.1 Introduction

For many metamorphic rocks is not a hard endeavor to infer or calculate the metamorphic peak *P-T* conditions, what can be done either by the presence of diagnostic mineral assemblages of restricted intervals of metamorphic temperature and using calculated petrogenetic grids (*e.g*. Spear & Cheney, 1989; Powell & Holland, 1990), or by calculation the intensive variables via conventional thermobarometry (*e.g.* Spear, 1989), multi-equilibrium methods (*e.g.* Powell& Holland, 1990), or using thermobarometry of trace elements in common or accessory minerals, such as Ti-in-quartz (Wark & Watson, 2006; Thomas *et al*., 2010), Zr-in-rutile (Zack *et al*., 2004; Watson *et al.*, 2006; Tomkins *et al*., 2007) and Ti-in-zircon (Watson *et al.*, 2006). However, the application of these techniques is restricted to rocks that have adequate bulk composition and, consequently, proper mineralogy, as pelites and mafic rocks. Furthermore, it is still desirable to relate the metamorphic temperature to the one of deformation. In some cases the relationship between porphyroblast growth and foliations is useful (Zwart, 1962; Passchier *et al*., 1992), but later deformation may obstruct this relationship or superpose it.

In many metamorphic terrains, quartzite is an abundant rock type, and until recently, not much could be done to use them to calculate or infer *P-T* conditions of deformation and metamorphism. Techniques for determining temperature of deformation and metamorphism of quartz-rich rocks start with recognition of recrystallization microstructures related to different mechanisms, as bulging, subgrain rotation and grain boundary migration, each of them related to different recrystallization/deformation temperatures (Kruhl, 1986; Passchier & Trouw, 2005) and also with the opening angle of the pattern formed in stereograms of quartz c-axis orientation (e.g. Kruhl, 1996; Law, 2014; Faleiros *et al*.., 2016). The bulging occurs at low temperatures, between 250 to 350 °C, where the grain edge suffers dislocations that reduce their size and produce the formation of subgrains and smaller grains at their edges (Stipp *et al.*, 2002). Recrystallization by subgrain rotation occurs at higher temperatures, between 350 and 450 °C and is characterized by the gradual change of subgrain orientation, by rotation of the crystal lattice of each subgrain until differences of their lattices are higher than 5-10° and new recrystallized grains are formed (Passchier & Trouw, 2005). Grain boundary migration occurs at temperatures higher than 450 °C, when the mobility of the contact between the grains happen and one grain end up consuming parts or whole other grains, whose lattice present unfavorable orientation (Passchier & Trouw, 2005). This kind of mechanisms is not uncommon to produce the increase in the average grain size in the rock (Passchier & Trouw, 2005).

The works presented by Kruhl (1986, 1996) are the pioneers in the subject, with determination of the relationship between textures, deformation mechanisms and temperature, in which quartz crystals were deformed. Quartz crystals are trigonal, and have a prismatic axis with greatest elongation, <c>, and basal, lower elongation, <a> (Kruhl, 1986). Recrystallization of the quartz crystals is the product of the ratio of high tensions over the rock and temperature. Thus, the higher the strain rate, the more intense is quartz deformation. In addition, the c-axis is affected mainly by higher temperatures and tensions, while the basal axis, <a> at lower temperatures and tensions (Kruhl, 1986). A first semi-quantitative attempt for a quartz c-axis thermometer is based on the recrystallization texture of quartz crystals and was already recognized the influence of strain rate and c-axis response (Kruhl, 1986).

Recently calibrations of a thermometer based on the opening angle formed by concentration of quartz c-axis orientation in stereograms were proposed, first with a shorter range in the temperatures (Law, 2014) and then with a larger temperature window and possible influence of pressure (Faleiros *et al*., 2016). These thermometers yield the possibility to calculate deformation temperature for rocks without metamorphic index minerals. Moreover, one of the greatest advantage of these thermometers is the possibility to investigate if temperature of main quartz recrystallization, and hence the deformation, is the same as the metamorphic index minerals, if they are present in the quartzite or in adjacent rocks.

Recent calibration of trace elements thermometers, such as Ti-in-quartz and Zr-in-rutile are very useful for quartzites as well. The Ti-in-quartz thermometer is used by measuring the Ti content in quartz, which concentration is proportional to its crystallization temperature. Experimental calibrations for this thermometer had proven to be very reliable (Wark & Watson, 2006; Thomas *et al*, 2010). It is also recommended to have a rock saturated in Ti, to guarantee that, presence of rutile is required (Wark & Watson, 2006; Thomas *et al.*, 2010). Another thermometer is Zr-in-rutile, as the concentration of Zr increases with temperature, and Zr replaces Ti on rutile structure, this produces a good thermometer (Zack *et al*., 2004). Tomkins *et al*., (2007) calculated a Zr-in-rutile thermometer that considers the effects of pressure to calculate the corresponding temperature.

The present paper aims to establish the relationship of the temperature of metamorphism and deformation of quartz-rich rocks, where a previous metamorphic history is already known. For this, a combination of quartz c-axis thermometer, including universal stage and EBSD analyses, Ti-in-quartz and Zr-in-rutile were applied to a sequence of quartzite which underwent progressive metamorphism. The rocks of the Carrancas Group, southern Minas Gerais, Brazil, were used for this investigation.

2.2 Geological Setting

The investigated rocks belong to Carrancas Group (Trouw *et al.*, 1983), that crop out in some nappes and klippen, in the southern Minas Gerais, Brazil, part of the Southern Brasília Orogen (Figure 14), which borders the eastern and southern portions of the São Francisco Craton (Campos Neto *et al.*, 2004, 2011).

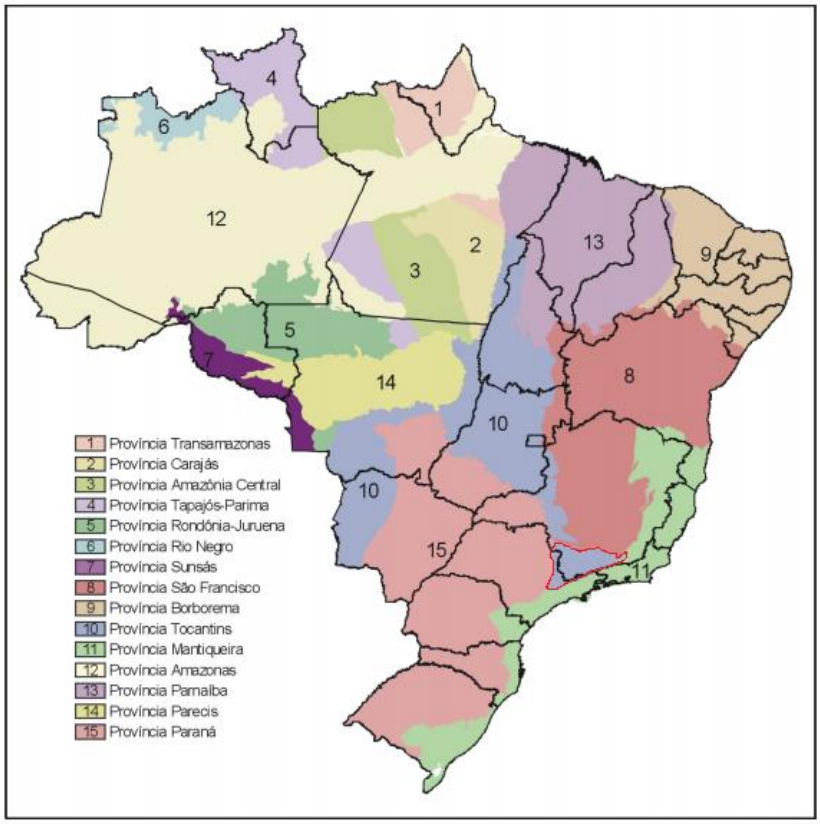

Figure 14: The main Structural Provinces of Brazil, with the Southern Brasília Orogen in red. (Modified by Bizzi *et al.*, 2003).

In this paper will be used the terminology made by Campos Neto *et al*. (2004, 2011) to indicate the geological depositional history as the Carrancas Group being part of the Carrancas Nappe System, which is a domain that belongs to the active margin of the Southern Brasília Orogen (Figure 15).

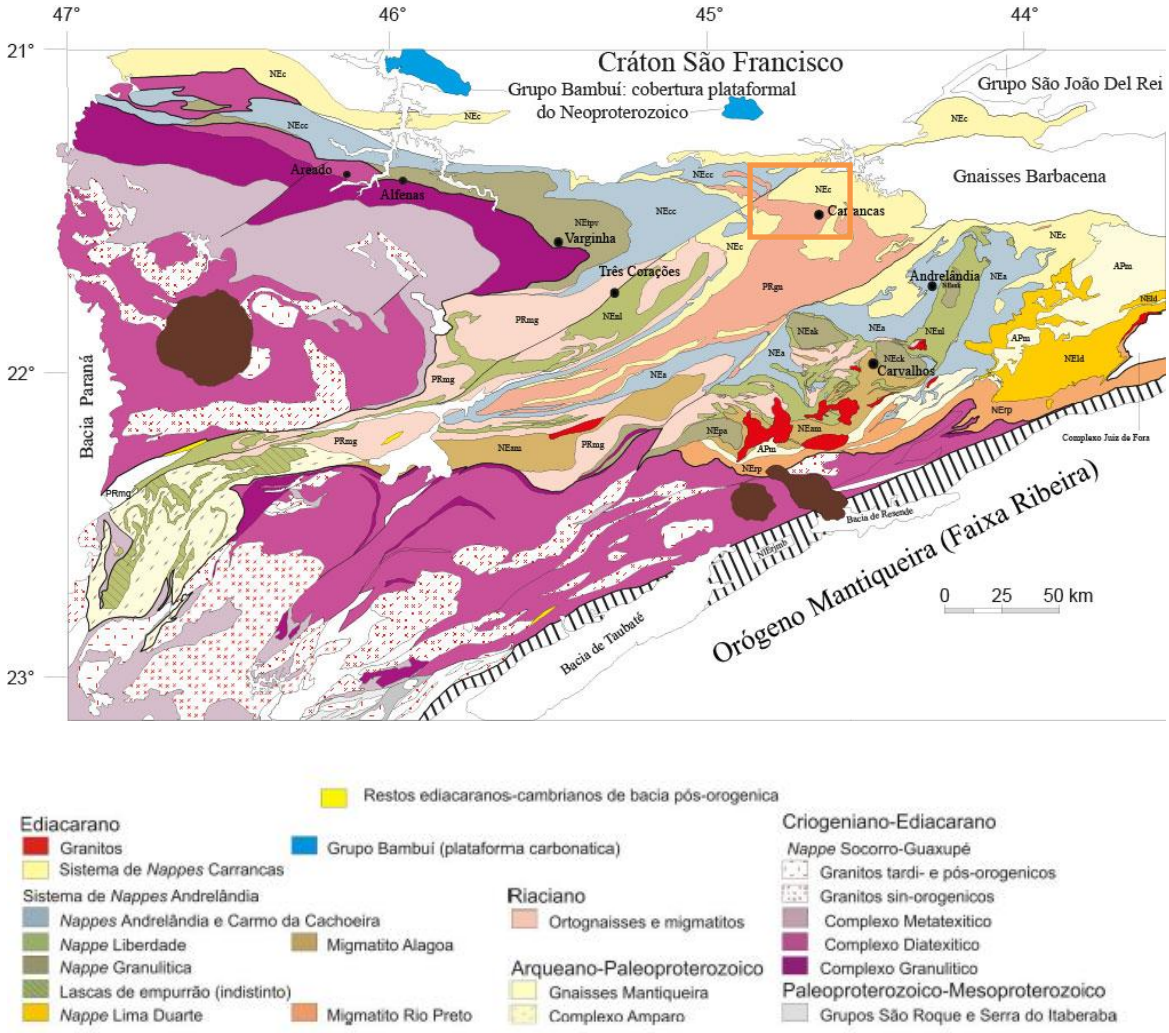

Figure 15 Simplified geological map of the Southern Brasília Orogen (according to Campos Neto *et al.*., 2011), in which the the box shows the study area.

The Carrancas Group crops out in well-defined geomorphological hills (Trouw *et al.*, 1983), called Serra do Pombeiro, Serra da Estância and Serra de Carrancas (Figure 16). It was originally divided into two formations, from the bottom to the top, São Tomé das Letras and Campestre (Ribeiro & Heilbron, 1982), after that it was added the Chapada das Perdizes Formation (Coutinho, 2012). The São Tomé das Letras Formation is composed of muscovite quartzite, with black tourmaline, rutile, Fe-Ti oxides, zircon, apatite, monazite with rare kyanite and microcline. Lenses of muscovite-quartz schist and muscovite schist are common. In direction to the structural top, it transitions to the Campestre Formation, made of interbedded phyllite or schist, with or without graphite, and quartzite with white mica (Ribeiro & Heilbron, 1982; Trouw *et al*., 1983). From north to south, the phyllite is replaced by schist, it gets coarser-grained and its mineralogy changes (Silva, 2010). Recently it was

proposed the top quartzite package, micaceous or not, is a different unit, named as Chapada das Perdizes Formation, which is identical to the one of the São Tomé das Letras (Coutinho, 2012).

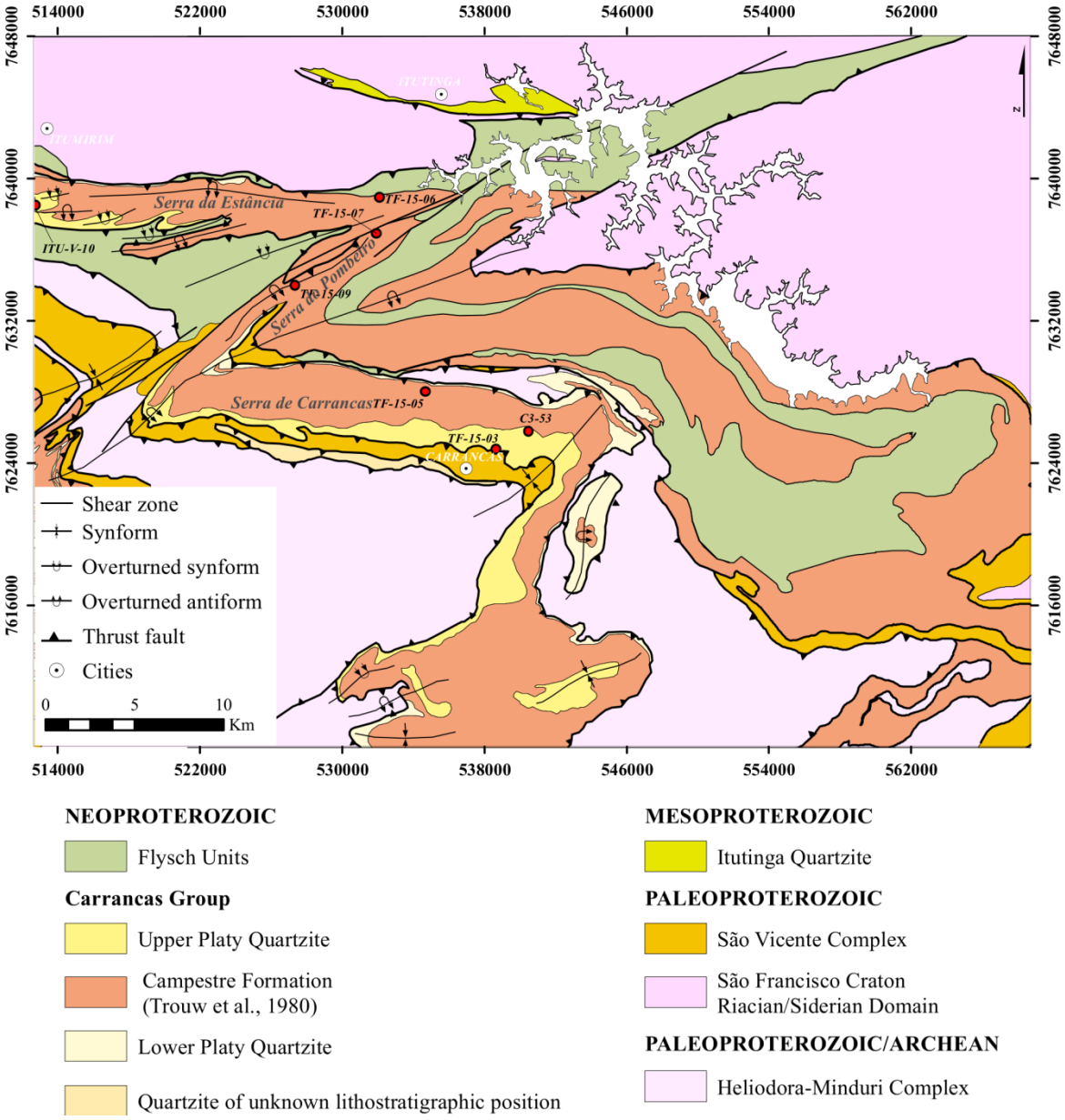

Figure 16: Geological map of the Carrancas region, with the samples location, including Serra da Estância, Serra de Carrancas and Serra do Pombeiro. Modified from Paciullo *et al*. (2002), Ribeiro *et al*. (2002) and Westin (2015).

In previous works, metamorphism was characterized as barrovian type, with the presence of almandine, staurolite and kyanite zones and temperature increasing from north to south, reaching its peak during the second phase of deformation (Trouw *et al*., 1983). Three metamorphic isograds were identified, garnet- and staurolite-in and chloritoid-out (Ribeiro &

Heilbron, 1982). A detailed work using pseudosections and thermobarometry confirmed the progressive character of metamorphism from north to south, as described earlier, but calculated pressures are higher than typical barrovian metamorphism. At its northern portion, at the Serra da Estância, peak metamorphic conditions of 586 ± 2 °C and 10.6± 0.6 kbar were determined, in the Serra de Carrancas, 620 ± 5 °C and 12.2 ± 0.5 kbar (Silva, 2010), whereas in the Serra das Bicas, 641 ± 35 °C and 11.2 ± 2.2 kbar (Garcia, 2010). In these three locations, mineral assemblages are formed by chloritoid + staurolite + chlorite, then garnet + kyanite + staurolite and garnet + kyanite + biotite, always with muscovite and quartz in excess.

2.3 Petrography

The São Tomé das Letras Formation of Carrancas Group is represented by muscovite quartzite and the muscovite quartzite interbedded with phyllite and muscovite-schist occur at the Campestre Formation.

The metapelites of Carrancas Group are distinguished by their granulometry and vary from phyllite to schist, from north to south. Phyllite and schist have almost the same mineral assemblage made up by muscovite, quartz, garnet porphyroblasts, varying from 0.3 cm to 0.6 cm, staurolite, kyanite, and both minerals ranging between 0.3 mm to 1.5 mm. Chloritoid occurs exclusively in phyllite, and rare biotite and fibrolite only occur in schist; porphyroblasts in the schist are much larger than in phyllite. The accessory minerals are rutile, monazite, zircon, tourmaline, epidote and opaque minerals.

The muscovite marks two foliations, S1, (in yellow), and S2, (in red - Figure 17). The garnet was formed prekinematic to synkinematic in relation to S2 (A and B; Figure 17). The same can be told about the kyanite and the staurolite grains, once they follow the muscovite foliation. In some samples there are quartz veins, interbedded with muscovite, with variety of thickness (C and D; Figure 17).

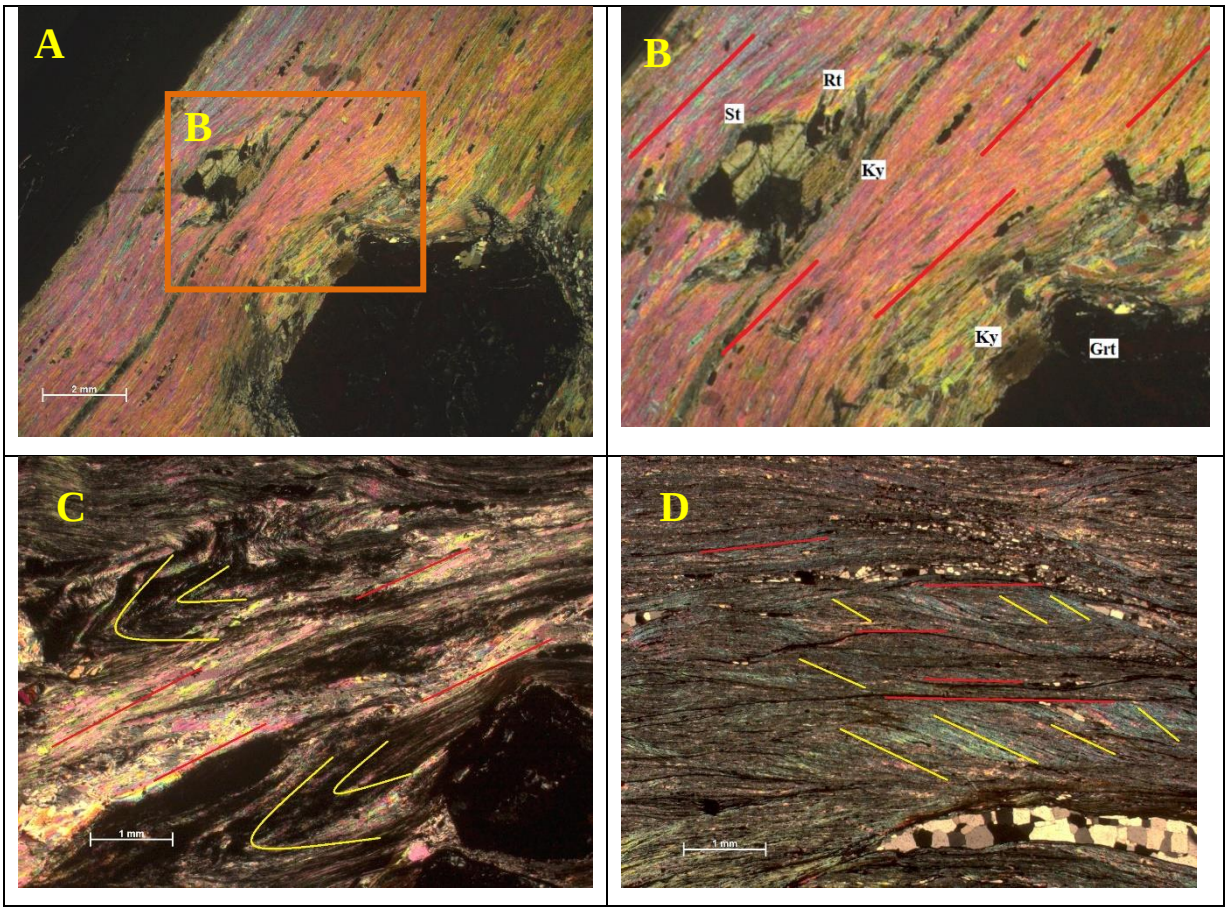

Figure 17: (A) and (B) are a thin section of schist. (C) and (D) shows both foliations observed on the schists of the Carrancas group; yellow is the S1 and red is the S2.

The quartzite of Carrancas Group is fine- to medium-grained, and contains variable proportions of feldspars, muscovite and accessory minerals, such as rutile, zircon, tourmaline, epidote and opaque minerals. Quartzite with more muscovite content develops shaper foliation, and muscovite along quartz defines the lineation. Two types of quartzite are identified based on the texture variation and distinct quartz microstructures. The first type has low amount of muscovite (up to 15%), which poorly defines the main foliation (D1; Figure 18 A-D). Muscovite is fine-grained, between 0.03 mm and 0.3 mm, and typically subdioblastics. Quartz grains (65%) are larger, 0.1 mm to 3.0 mm, and have curved to embayed contacts.

In the second type, muscovite makes up to 35% of modal proportion in the rock, with well-formed placoid crystals, forming oriented lenses and defining the main foliation of the rock (Figure 18 E-H), and quartz 65%. Quartz grains vary in size due to the influence of contacts with muscovite, which limits their size (Figure 18A). The muscovite-richest layers, quartz grains are fine-grained, between 0.03 mm and 0.5 mm, and in the muscovite-poorest ones, quartz are bulky, between 0.02 mm and 1.5 mm.

Both types of quartzite described in this work have opaque minerals and rutile as accessory minerals (less than 5%).

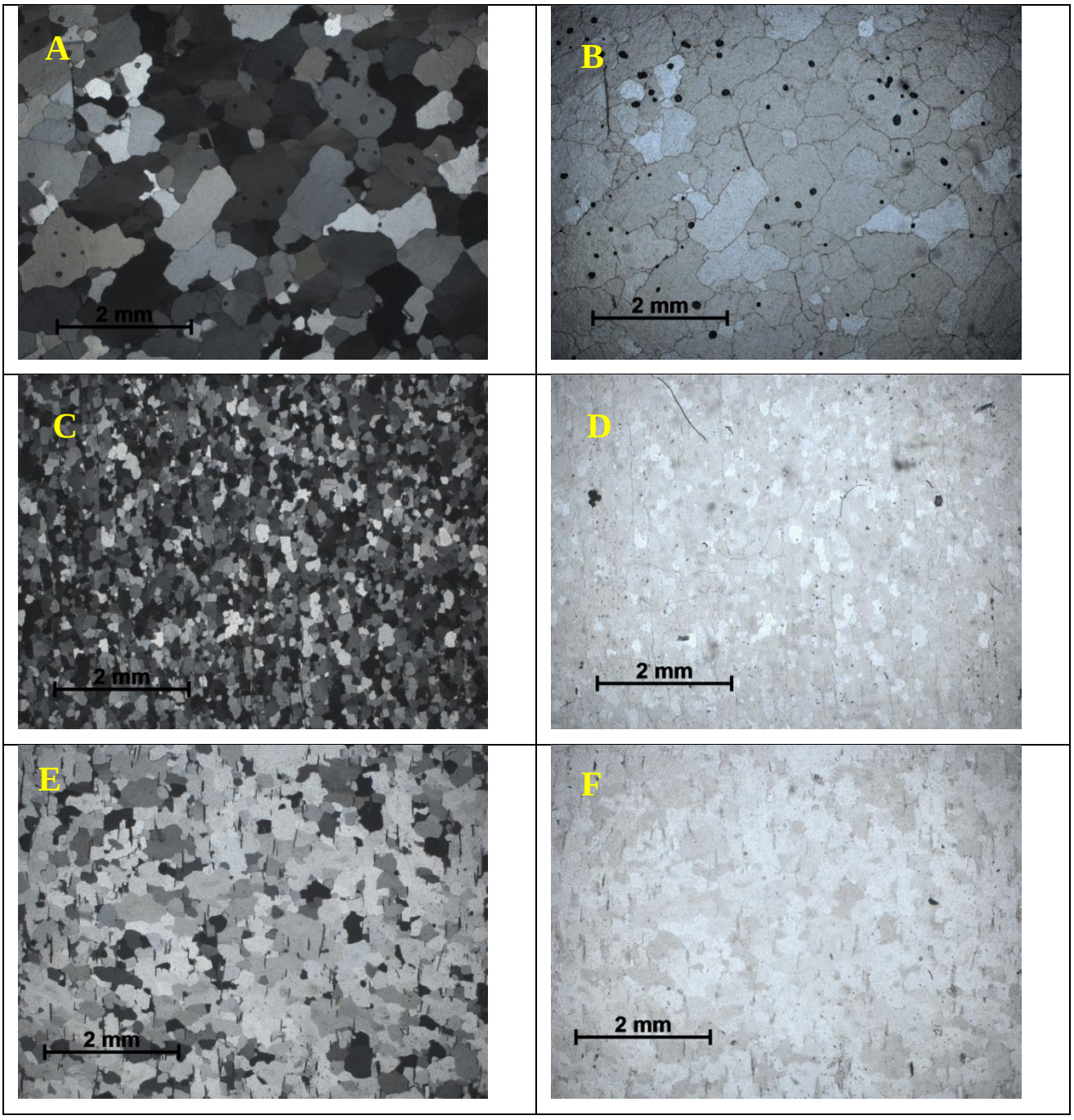

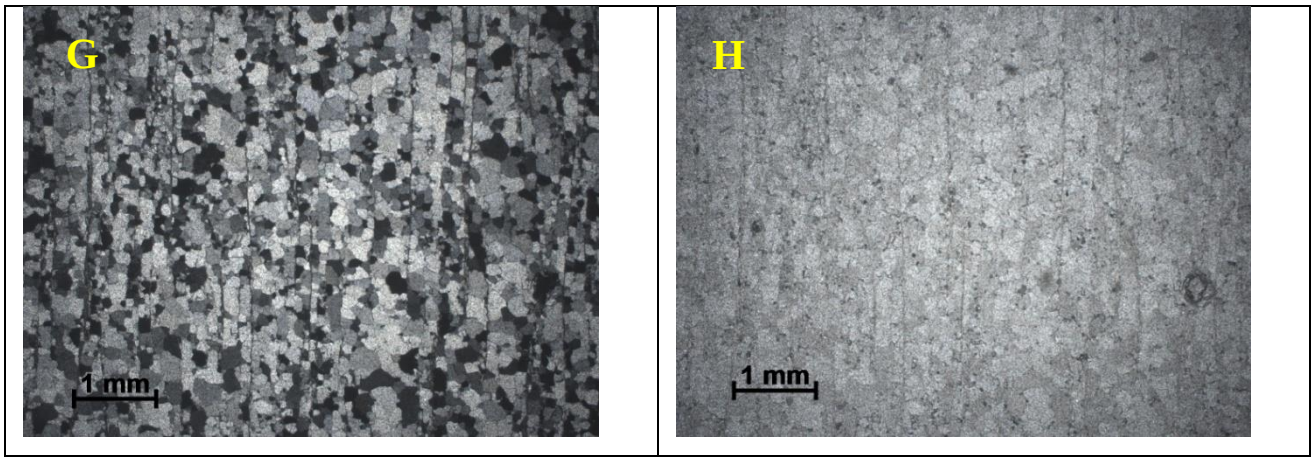

Figure 18: Photomicrographs of the thin sections analyzed. (A) and (B) are from samples C3-53 and (C) and (D) from TF-05-07, showing the low percentage of muscovite on the matrix. (E), from TF-15-03, and (F), from TF-15-06, shows the lineation and the quartz recrystallization controlled by the presence of muscovite. (G) and (H), from TF-15-06, shows the morphology of the rutile on the quartzite rocks. All of the rocks have rutile as an accessory mineral.

There are two main foliations in the study samples, one developed by the orientations of muscovite (D1; Figure 19), and the other one, by the orientation of quartz and muscovite (D2; Figure 19). In the samples where muscovite defines the main foliation, it also delimits the recrystallization size of quartz grains (A and B, Figure 19). It is noticed, because the difference of size of the quartz grains is very perceptive once there is muscovite on the thin section, the quartz grains have straight contacts with the first and is smaller, between 0.03 mm and 0.5 mm, while in the samples that have no muscovite, quartz grains are larger.

The bulging is the first stage of dynamic recrystallization on quartz grains, and of the products is the ‘left-over grains’, the grains that had their boundaries migrated into smaller grains (B, Figure 19).

The more advance stage of static recrystallization, the more the boundaries of the minerals are straight, in other words, there were more grain boundary migrations, and the temperature of recrystallization is higher in these samples (E, Figure 19).

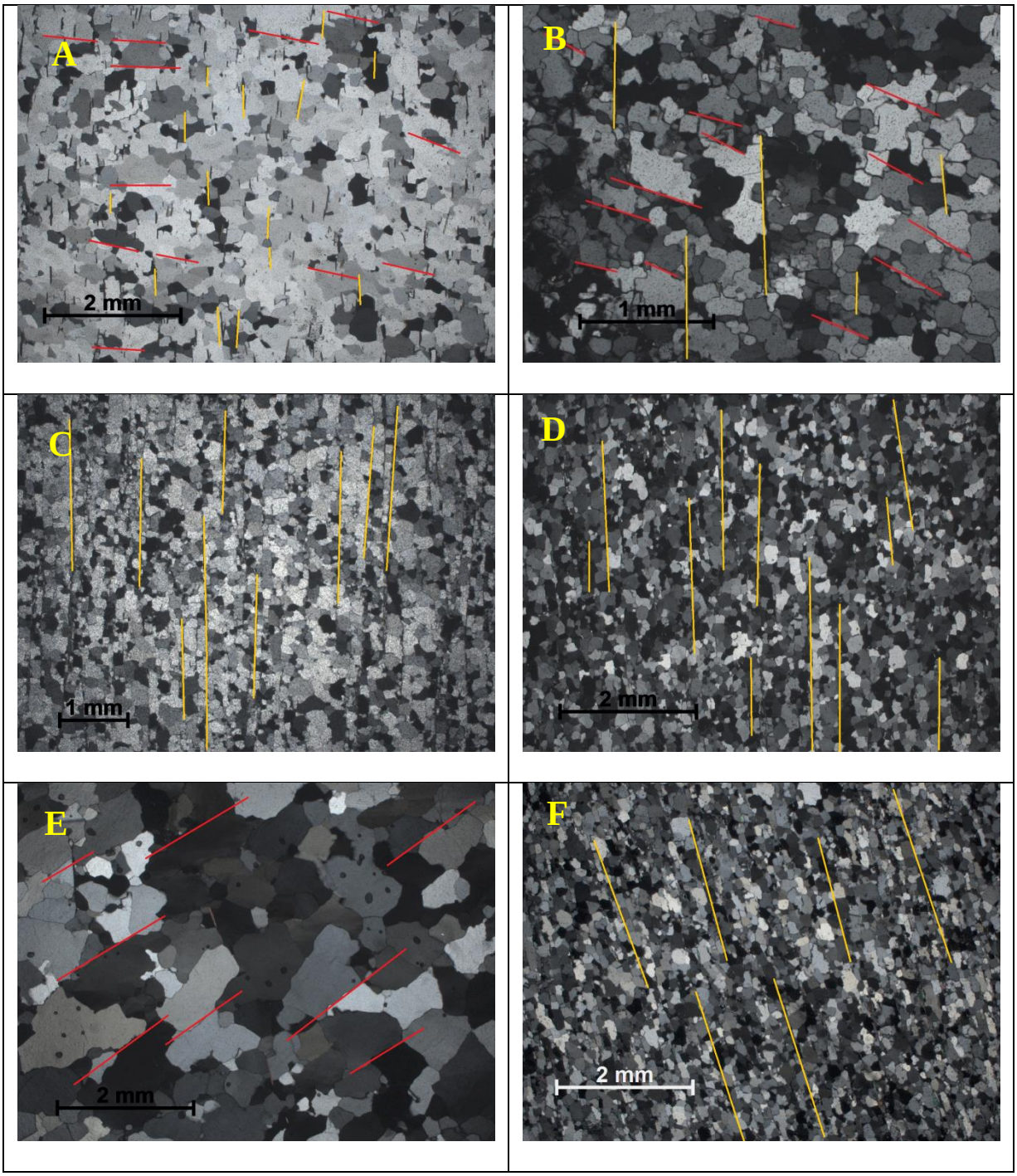

Figure 19: Figures from TF-15-03(A), TF-15-05 (B), TF-15-06 (C), TF-15-07(D), C3-53(E), ITU-V-10(F). Figures (A), (B) shows the main foliation defined by muscovite, yellow lines, and the second foliation defined by the stretch of quartz minerals, red lines. Figures (C), (D), and (F) shows only the lineation defined by muscovite, and figure (E) shows only the lineation defined by quartz.

2.4 Universal Stage and Electron Backscatter Diffraction (EBSD)

Seven samples were analyzed on universal stage, and an average of 300 measurements of c-axis tilt of quartz crystals were obtained, and on EBSD for comparison purposes. The

universal stage data was compiled using a Leitz Wetzlar petrographic microscope with a coupled universal stage. The EBSD analyses were performed on a Tescan Mira 3 FEG SEM, with the detector from Oxford Instruments Nordlys NANO, in the LAME-LACTEC laboratory from the Federal University of Paraná (UFPR) with the following conditions: acceleration voltage between 15 and 25 kV; 18 µA; sample detector distance of 18 mm; step size varying for each sample, near 10% of the grains average size. The software for post processing results is the Channel 5 from Oxford Instruments.

The open source Matlab® toolbox MTEX was used to quantify pole figure symmetries (Bachmann *et al*., 2010), and to generate the opening angles girdles it was used the Hunter *et al*., (2018) script, eliminating the subjectivity that comes with qualitative pole figure analytical methods (Hunter *et al*., 2018). Temperatures were calculated with the opening angles and using the Faleiros *et al*., (2016) geothermometric calibrations.

The universal stage results are presented in figure 20 and table 1 has the information about location, symmetry, opening angle and temperature for each sample.

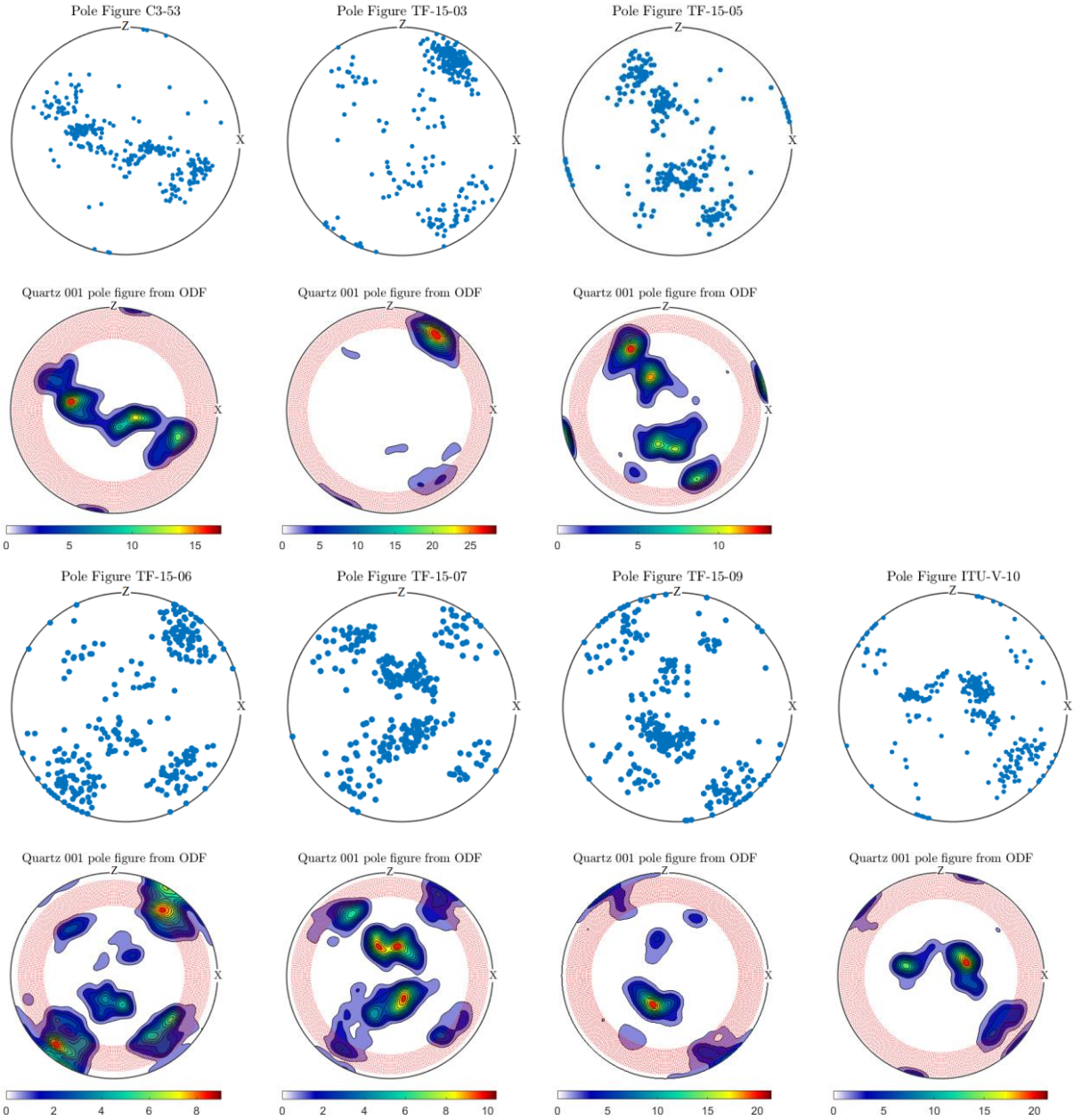

Figure 20: Quartz c-axis measures taken on the universal stage. 300 measures were gathered from each sample. Pole Figures and Orientation Density Function (ODF) images, made with MTEX script by Hunter *et al*. (2018), with the area (red band) of calculation of the Opening Angles (OA) on stereogram with c-axis projected on lower hemisphere.

Table 1: Opening angles and symmetries obtained using Hunter *et al*. (2018) MTEX script and temperatures using Faleiros *et al*. (2016) calibration. The pressure values are from Silva (2010) for the Serra da Estância and Garcia (2010) for the Serra de Carrancas and Serra do Pombeiro.

Samples	Location	*P* (kbar)	Symmetry (*S*)	OA (Degrees)	*T* (°C)	±
C3-53	Serra de Carrancas	11.16	0.2374	77.5	672.25	50
TF-15-03	Serra de Carrancas	11.16	0.2176	63.5	590.45	50
TF-15-05	Serra de Carrancas	11.16	0.1265	68.5	621.60	50
TF-15-07	Serra do Pombeiro	10.65	0.7604	72.5	637.60	50
TF-15-09	Serra do Pombeiro	10.65	0.1901	58.5	549.55	50
TF-15-06	Serra da Estância	10.65	0.3386	78.5	670.25	50
ITU-V-10	Serra da Estância	10.65	0.3525	73	640.40	50

The MTEX script estimates the degree of girdle symmetry, being *S*=1 a very symmetric pole figure, for relative contributions of coaxial (orthorrombic) and, *S*=0, non-coaxial (monoclinic) deformation modes (Hunter *et al*., 2018). For the samples C3-53, TF-15-03 and TF-15-05, of Serra de Carrancas, the symmetry ranges from *S*=0.1265 (TF-15-05) to *S*=0.2374 (C3-53), therefore being very asymmetric and leaning to non-coaxial deformation. From Serra do Pombeiro TF-15-09 is very asymmetric (*S*=0.1901) and the TF-15-07 is much closer to a symmetric pole figure (*S*=0.7604), being the most symmetrical pole figure of all of the samples, and registering a more coaxial deformation. Yet, the samples from the Serra da Estância have very similar results, *S*=0.3386 (TF-15-06) and 0.3525 (ITU-V-10), ranked as non-coaxial deformation.

The temperatures of the pole figure, gathered from the Universal Stage analysis, were obtained applying the Faleiros *et al*. (2016) calibration with the opening angle generated by the MTEX script (Hunter *et al*., 2018). From the Serra da Estância, the temperatures varied from 640 °C ± 50 (ITU-V-10) to 670 °C ± 50 (TF-15-06). The Serra do Pombeiro calculated temperatures varied from 549 °C ± 50 (TF-15-09) to 637 °C ± 50 (TF-15-07) and for Serra de Carrancas varied from 590 °C ± 50 (TF-15-03) and 672 °C ± 50 (C3-53).

It is expected that the advantage of using the EBSD over universal stage is the higher amount of collected data, giving a better statistical meaning for the analysis (Fazio *et al*., 2017), as it is an automated technique and gives thousands of measurements. The EBSD results are given at figure 21 and table 2, where the number of measurements of each sample varied between 1200 and 250000, but it was preferred to generate pole figures with 25000, which result into a clearer image for girdle symmetry identification. Stereogram presents the distribution of the measurements and the symmetry of the girdle (*S*).

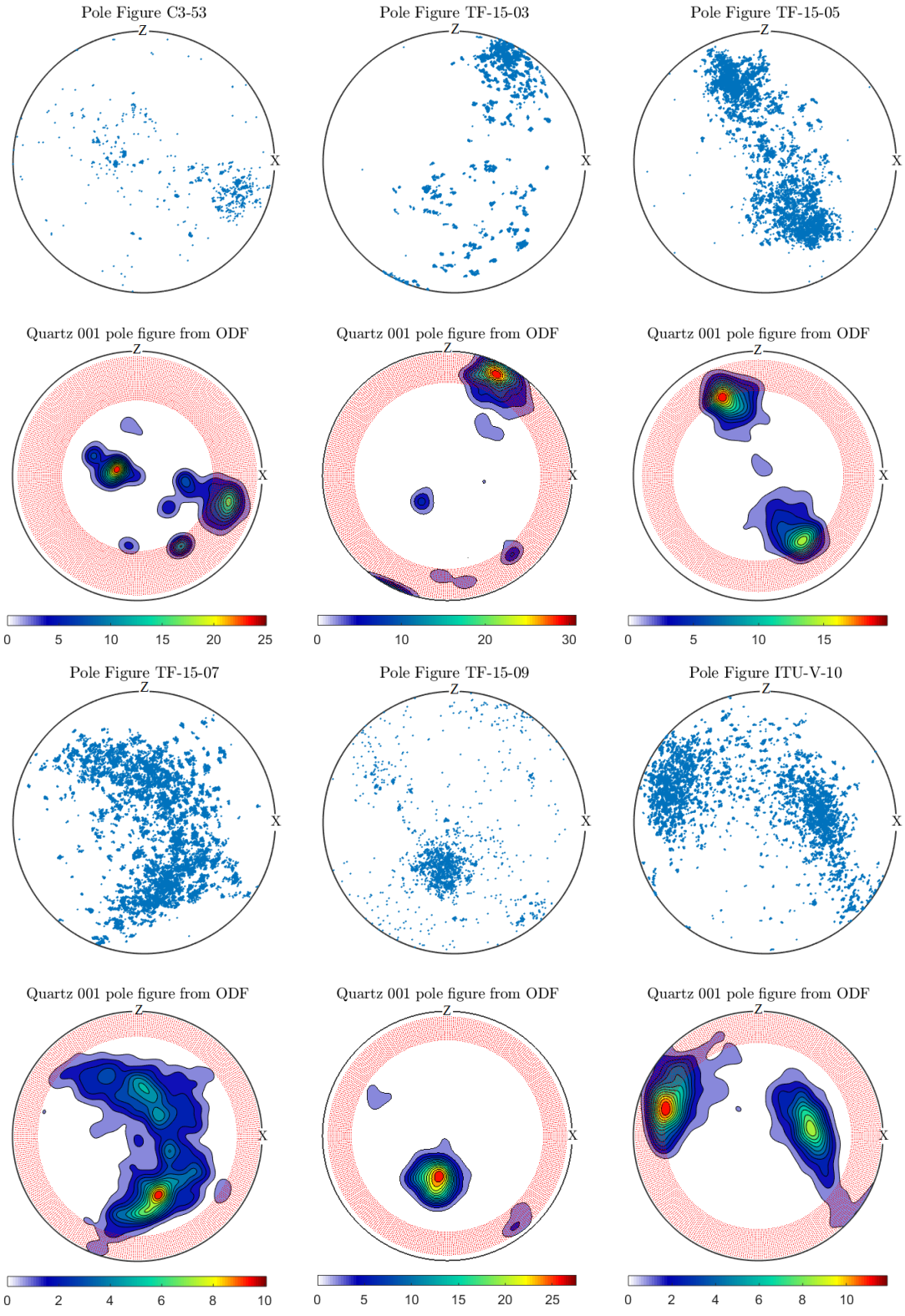

Figure 21: Quartz c-axis measures taken on the universal stage. 25000 measures were plotted from each sample. Pole Figures and Orientation Density Function (ODF) images, made with MTEX script by Hunter *et al*. (2018), with the area (red band) of calculation of the Opening Angles (OA) on stereogram on lower hemisphere.

Table 2: Opening angles and symmetries obtained using Hunter *et al*. (2018) MTEX script and temperatures using Faleiros *et al*. (2016) calibration. The pressure values are from Silva (2010) for the Serra da Estância and Garcia (2010) for the Serra de Carrancas and Serra do Pombeiro.

Samples	Location	*P*(kbar)	Symmetry (*S*)	OA (Degrees)	*T*(°C)	±
C3-53	Serra de Carrancas	11.16	0.1831	71	636.27	50
TF-15-03	Serra de Carrancas	11.16	0.2826	44.5	444.52	50
TF-15-05	Serra de Carrancas	11.16	0.0006	70	630.45	50
TF-15-07	Serra do Pombeiro	10.65	0.7122	80	678.00	50
TF-15-09	Serra do Pombeiro	10.65	0.4523	65	592.78	50
ITU-V-10	Serra da Estância	10.65	0.0975	91.5	733.13	50

For the results of EBSD, the symmetry of the samples for Serra de Carrancas varied from 0.0006 (TF-15-05) to 0.2826 (TF-15-05), giving a highly asymmetrical set of girdles and non-coaxial deformation. The samples of Serra do Pombeiro varied from 0.4532 (TF-15-09) to 0.7122 (TF-15-07), where the highest value gives a more symmetrical girdle, registering a coaxial deformation. The sample ITU-V-10, from Serra da Estância, has an *S* value of 0.0975, which is highly asymmetrical.

The temperatures of the pole figure, gathered from the EBSD analysis, were obtained applying the Faleiros *et al*. (2016) calibration with the opening angle generated by the MTEX script (Hunter *et al*., 2018). From the Serra da Estância, the temperature is 733 °C from sample ITU-V-15, for Serra do Pombeiro the temperatures varied from 592 °C (TF-15-09) to 678 °C (TF-15-07) and for the Serra de Carrancas varied from 444 °C (TF-15-03) to 636 °C (C3-53), all of them ± 50.

The girdles from Universal Stage stage are classified as type II and the EBSD pole figures are not symmetrical and asymmetrical for being classified as proposed by Faleiros *et al*. (2016) (Figure 22).

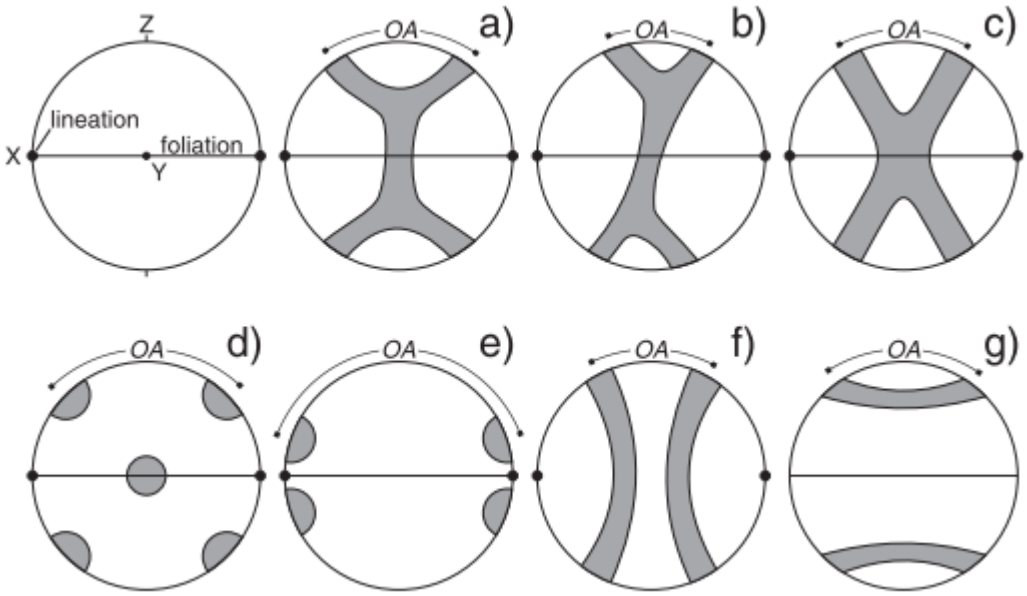

Figure 22: Common patterns of quartz c-axis fabrics with indication of the opening-angle (OA). X, Y, and Z are the main axes of the strain ellipsoid. (a) Symmetric type I crossed girdle. (b) Asymmetric type I crossed girdle. (c) Type II crossed girdle. (d) Point c-maxima in Y and intermediate positions between X and Z. (e) Point c-maxima at low angles to the stretching lineation (X). (f) Cleft girdle (constrictional strain). (g) Small circle distribution centered in the foliation pole (Z) (flattening strain) (Faleiros *et al.*, 2016)

2.5 Trace elements thermometer

The chemical composition of rutile was analyzed in the Geosciences Institute of São Paulo University, using a JEOL Electron Microprobe, model JXA-FE-8530, under conditions of 20 kV and 20 nA, with a beam diameter of 5 µm and natural minerals were used as standards for all elements. For analyses, the protocol established by Zack et al. (2004) was followed. Quartz was analyzed with a LA-ICP-MS, using an iCAP Q - Thermo Scientific coupled with a New Wave 213 A/F laser, a series of glasses of Heraeus, saturated with several elements were used as standards.

Temperature determinations were calculated on five different samples (Figure 8), being five (A; Figure 23) samples for Zr-in-rutile method and four (B; Figure 23) for Ti-in-quartz. For the Zr-in-rutile thermometer the calibration made by Tomkins *et al*. (2007) was used and, for the Ti-in-quartz, the Thomas *et al*. (2010) calibration was used, instead. The thermobarometer values were taken by previous studies, being 641 ± 35 °C and 11.16 ± 2,2 kbar for the Serra de Carrancas (Garcia, 2010) and 586 ± 2 °C and 10.65 kbar for the Serra do

Pombeiro and Serra da Estância (Silva, 2010). Considering the work by Ashley and Law (2015) and previous *P-T* estimations, the α_{TiO_2} ~1 is adopted in this work.

The box-plot (Figure 23) shows the data set collected on each analysis, Zr-in-rutile and Ti-in-quartz, where the length of the box is the interquartile and gives the range of the data set. The line across the box represents the median and the 'whiskers' expands to the outermost data point that lies 1.5 times the interquartile range beyond the edges of the box (Tomkins *et al.*, 2007). Also, Tomkins *et al*. (2007) proposes a reliable way of estimating the best temperature on Zr-in-rutile temperatures range on box-plot is to use temperature of the upper end of the box-plot.

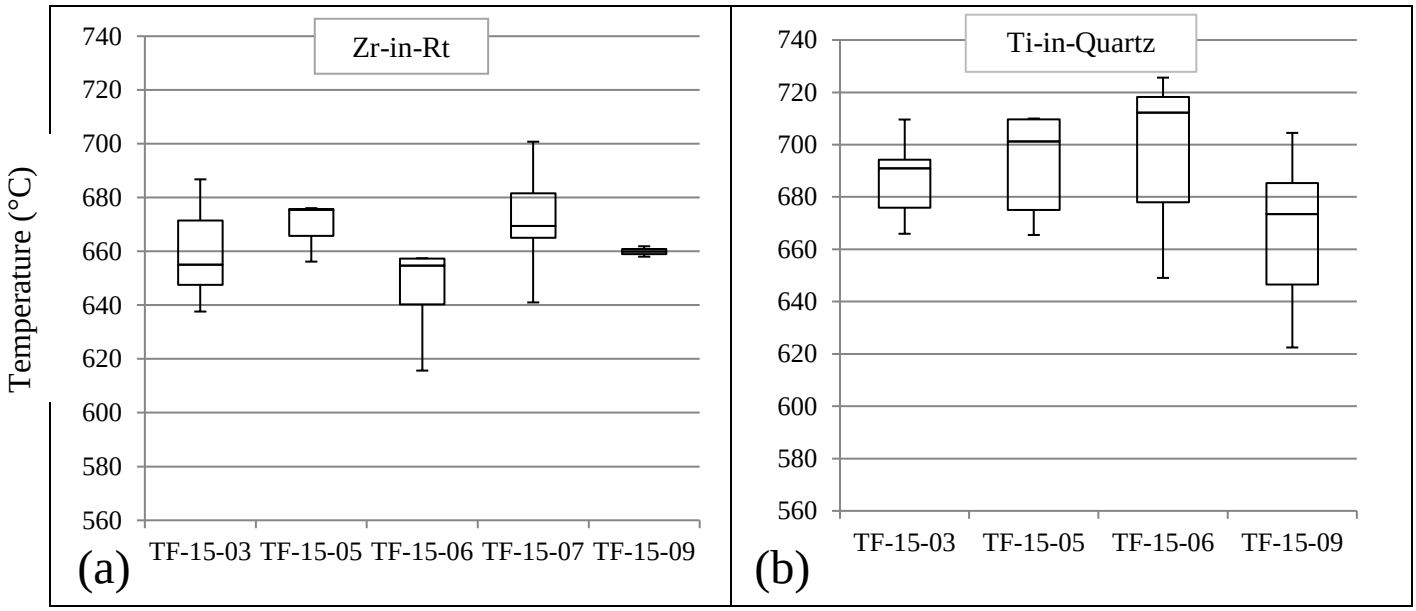

Figure 23: Zr-in-rutile results were obtained using Tomkins *et al*. (2010) calibration. Ti-in-quartz results were obtained using Thomas *et al*. (2007) calibration.

The temperatures obtained from the Ti-in-quartz thermometer for the Serra de Carrancas were, between, an average of 685 °C (TF-15-03) and 700 °C (TF-15-05), and the maximum temperature was 740 °C. For the average temperatures obtained using the Zr-in-rutile thermometer, for the same samples, were from 676 °C (TF-15-03) to 686 °C (TF-15-05), and the upper end of the box plot varied from 672 (TF-15-03) to 675 °C (TF-15-05).

The Serra do Pombeiro had an average of about 658 °C (TF-15-09) for the Ti-in-quartz thermometer, having the maximum temperature at 697 °C, and for the Zr-in-rutile the average temperatures ranged from 659 °C (TF-15-09) to 673 °C (TF-15-07), having the upper end of the box plot varying from 661 (TF-15-09) to 683 °C (TF-15-07).

For the samples from Serra da Estância, the average results from Ti-in-quartz thermometer was 705 °C (TF-15-06), the maximum temperature was 789 °C. The Zr-in-rutile thermometer gave an average of 651 °C (TF-15-06), having the upper end temperature of the box plot with 657 °C.

Table 3: Mean and maximum temperatures for Ti-in-quartz and average and upper end of the box-plot for Zr-in-rutile temperatures are compared.

sample	Location	P (kbar)	Ti-in-Quartz (°C)		Zr-in-Rutile (°C)	
			Average	Maximum	Average	Upper end
TF-15-03	Serra de Carrancas	11.16	685.11	713.71	659.42	672
TF-15-05	Serra de Carrancas	11.16	700,08	740.15	669.23	675
TF-15-07	Serra do Pombeiro	10.65	-	-	673.87	683
TF-15-09	Serra do Pombeiro	10.65	658.48	697.06	659.96	661
TF-15-06	Serra da Estância	10.65	705.83	789.78	651.32	657

Intercepting the Ti and Zr concentrations, in ppm, from quartz and rutile, respectively, on the same isopleths diagram proposed in Thomas *et al*. (2010), it is possible to determine *P-T* conditions for crystallization of quartz and rutile (Figure 24). For sample TF-15-03, the conditions are, approximately, 9.5 kbar and 655 °C (A, Figure 24); for sample TF-15-05, 9.7 kbar and 660 °C (B, Figure 8); for sample TF-15-06, 7.0 kbar and 640 °C (C, Figure 24) and for sample TF-15-09, 10.1 kbar and 650 °C (D, Figure 24). The red lines are the Zr-in-rutile concentrations and the purple is for Ti-in-quartz, where the mean concentrations are the middle lines and the dashed lines are maximums, on the right, and minimums, on the left.

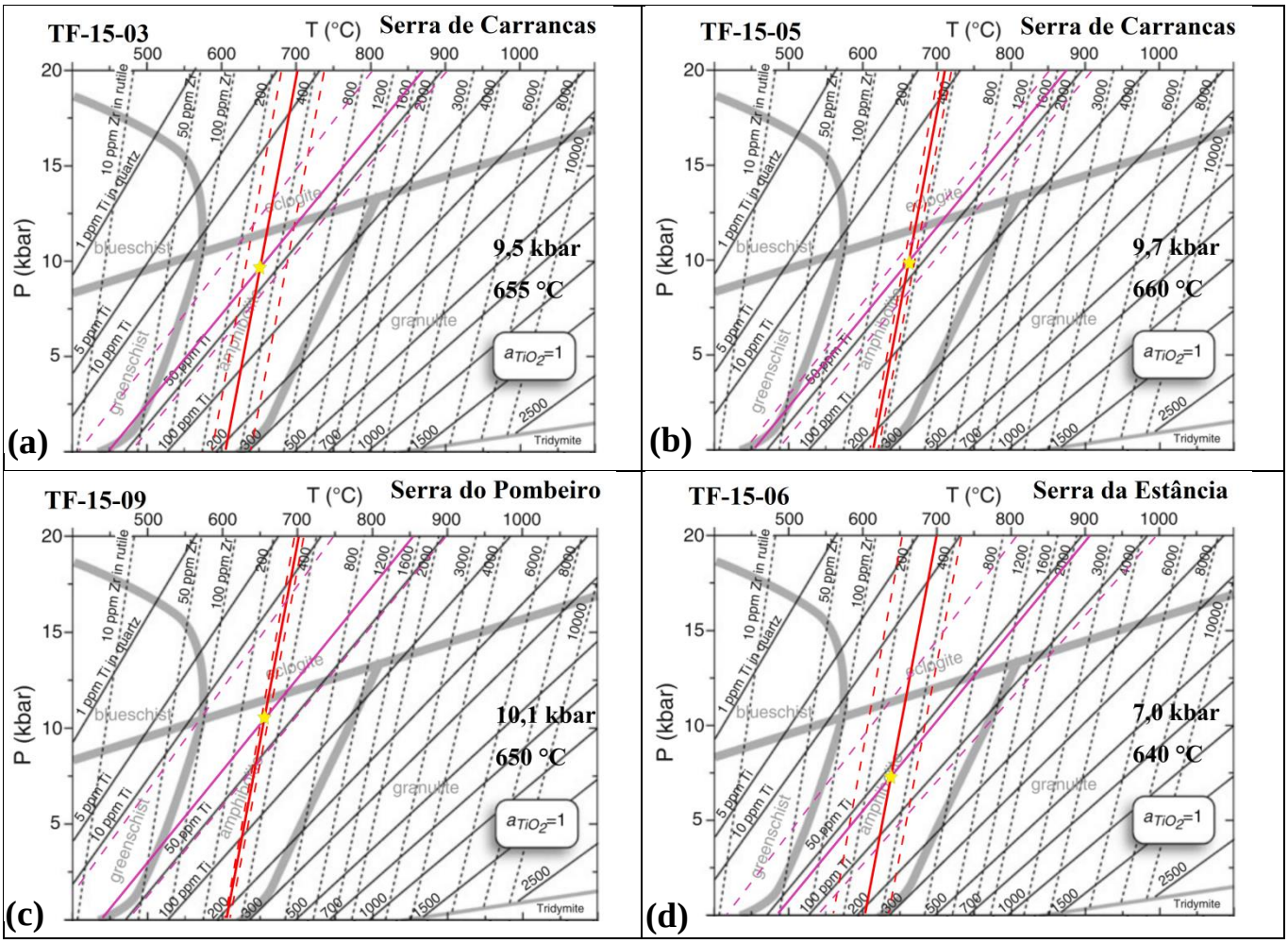

Figure 24: *P-T* diagrams intercepting Zr-in-rutile and Ti-in-quartz concentrations for samples (a) TF-15-03; (b) TF-15-05; (c) TF-15-06 and (d) TF-15-09 for investigate the crystallization conditions from South to North (Thomas *et al*., 2010).

CHAPTER 3 – DISCUSSIONS

The aim of this research is to use the c-axis quartz thermometer to investigate variations of metamorphism in an area where metamorphic conditions are known, in this case, the rocks of Carrancas Group in the homonymous region, to check how precise the thermometer can reproduce the conditions of peak of metamorphism or later stages of deformation. Combined with the c-axis thermometer, trace elements thermometers were used as well, Ti-in-quartz and Zr-in-rutile, for comparison purposes.

The metamorphism at Carrancas Group increases from North to South, so it was expected higher temperatures from Serra da Estância to Serra de Carrancas. The pressure values used in the above table were taken from Silva (2010) for the rocks of Serra da Estância and Pombeiro, which calculated for the former, by thermobarometry a temperature of 586 ± 2 °C and a pressure of 10.65 ± 0, 45 kbar. Garcia (2010) calculated, by the same method, the temperature and pressure for the rocks of the Serra das Bicas, corresponding to 641 ± 35 °C and 11.16 ± 2.2 kbar, which were used for Serra de Carrancas because the rocks are from the same metamorphic zone as the ones investigated here.

3.1 Universal Stage and Electron Backscatter Diffraction

When the results of the opening angle calculated with Universal Stage and Electron Backscatter Diffraction (EBSD) are compared, even though they are calculated using the same script created by Hunter *et al*. (2018), they produced different results than expected for the same samples. Even if the Universal Stage analyses were performed only with 300 measurements and considering it has an uncertainty from the manual instrumentation, it is consider being statistically acceptable for obtaining reliable results. Taking these facts in consideration, the opening angle results are within the standard deviation of 50 °C (Tables 1 and 2), and the girdles, obtained with the pole figures, were different for each technique, which was not expected because of the high density number of measurements the EBSD scanned. Another way for comparing the Universal Stage and EBSD c-axis fabrics is to use the symmetry results for each sample. For both techniques, the symmetries were alike, for the exception of the sample TF-15-03, where the symmetry for Universal Stage is 0.1265 and, for the EBSD, 0.0006 (Tables 1 and 2).

The average temperature for Universal Stage analysis obtained for the Serra de Carrancas is 628 °C, for the Serra do Pombeiro, 593 °C and, for the Serra da Estância, 655 °C. The average temperature for the EBSD for the Serra de Carrancas is 570 °C, for the Serra do

Pombeiro 635 °C, and for Serra da Estância, 733 °C. Comparing the Universal Stage results with the thermobarometry of previous studies, the average temperature for Serra da Estância does not agree with the temperature of 586 ± 2 °C (Silva, 2010), and it is the highest average temperature of the three study areas. Correlating the EBSD results with the thermobarometry of previous results, all the samples gave higher temperatures, not corresponding to what was expected and predicted with mineral assemblages: grade of metamorphism to get higher from north to south (Table 3).

Table 4: Comparison of the results of opening angles and temperatures for Universal Stage and EBSD analysis.

sample	Location	P (kbar)	Universal Stage		EBSD	
			OA	T °C	OA	T °C
C3-53	Serra de Carrancas	11.16	77.5	672.25	71	636.27
TF-15-03	Serra de Carrancas	11.16	63.5	590.45	44.5	444.52
TF-15-05	Serra de Carrancas	11.16	68.5	621.60	70	630.45
TF-15-07	Serra do Pombeiro	10.65	72.5	637.60	80	678.00
TF-15-09	Serra do Pombeiro	10.65	58.5	549.55	65	592.78
TF-15-06	Serra da Estância	10.65	78.5	670.25	-	-
ITU-V-10	Serra da Estância	10.65	73	640.40	91.5	733.13

Since there are two main foliations on the quartzite (Figure 5), one determined by the muscovite and the other one by the quartz grains orientation, the temperatures from the EBSD could have overlapped all the quartz-c axis tilts giving a higher and less precise temperature, even though it is statistically more representative than quartz-c axis fabrics from Universal Stage measurements. The advantage of the Universal Stage technique is to choose each grain for making up a trustworthy stereogram on each foliation observed on petrography. Even though this was observed on the results, an important factor for the difference of the temperatures for Universal Stage and EBSD could be the superimposed shear zone among the Serra de Carrancas, which is from W-E direction. Other reason could be the lack of mastery on this analysis results being a restraint for the interpretation of the EBSD data.

3.2 Trace elements thermometer

The temperatures gathered by the trace elements thermometer were higher than the *P-T* conditions obtained by Silva (2010) and Garcia (2010). The Ti-in-quartz temperatures were higher than the Zr-in-rutile, as seen in figure 23, and comparing along the location of each sample, there is no direct correlation with the prograde metamorphism from North to South

described on the literature. Also, for each sample, there is a large temperature variation that may raise que question if the Zr-in-rutile reach proper equilibrium in these samples to be used in a reliable way.

Since zircon behaves as an inactive phase on rocks with temperatures lower than 600 °C (Cruz-Uribe *et al.*, 2018), the Zr-in-rutile temperatures for Serra do Pombeiro and Serra da Estância might present the detrital composition from the source rock or non-fully equilibrated temperatures providing an unreliable result (Figure 25). For Serra de Carrancas, since the thermobarometry gives a temperature of, approximately, 641 °C (Garcia, 2010), the rutile registered a more reliable temperature of crystallization and interaction with quartz but still with a very large spread in the calculated temperature.

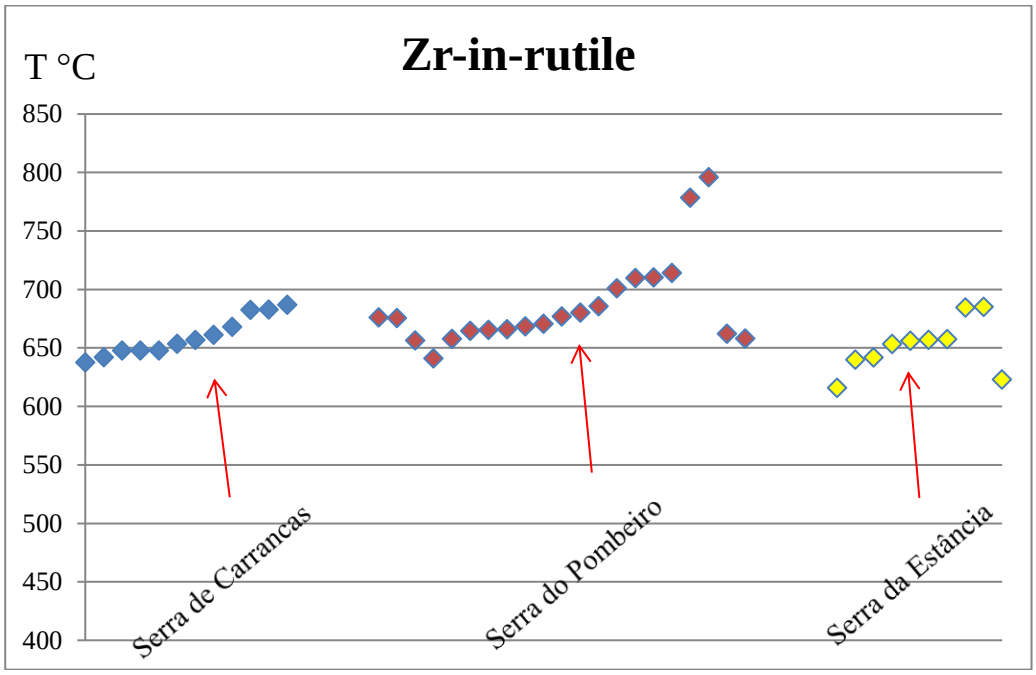

Figure 25: Zr-in-rutile temperatures calculated using calibration by Tomkins *et al.* (2007). The blue temperatures are from Serra de Carrancas from samples TF-15-03 and TF-15-05, the red temperatures from Serra do Pombeiro and are from samples TF-15-07 and TF-15-09, and the yellow temperatures are from Serra da Estância from sample TF-15-06.

The results from Ti-in-quartz thermometer might indicate that the quartz grains did not interact with rutile as much as necessary to equilibrate the Ti concentrations into its lattice, so it might have been trapped on quartz lattice and giving erroneous temperatures.

Comparing all the samples regarding analyses and the temperatures, the Universal Stage gave smaller results, followed by the EBSD, Zr-in rutile and, finally, the Ti-in-quartz (Figure 26).

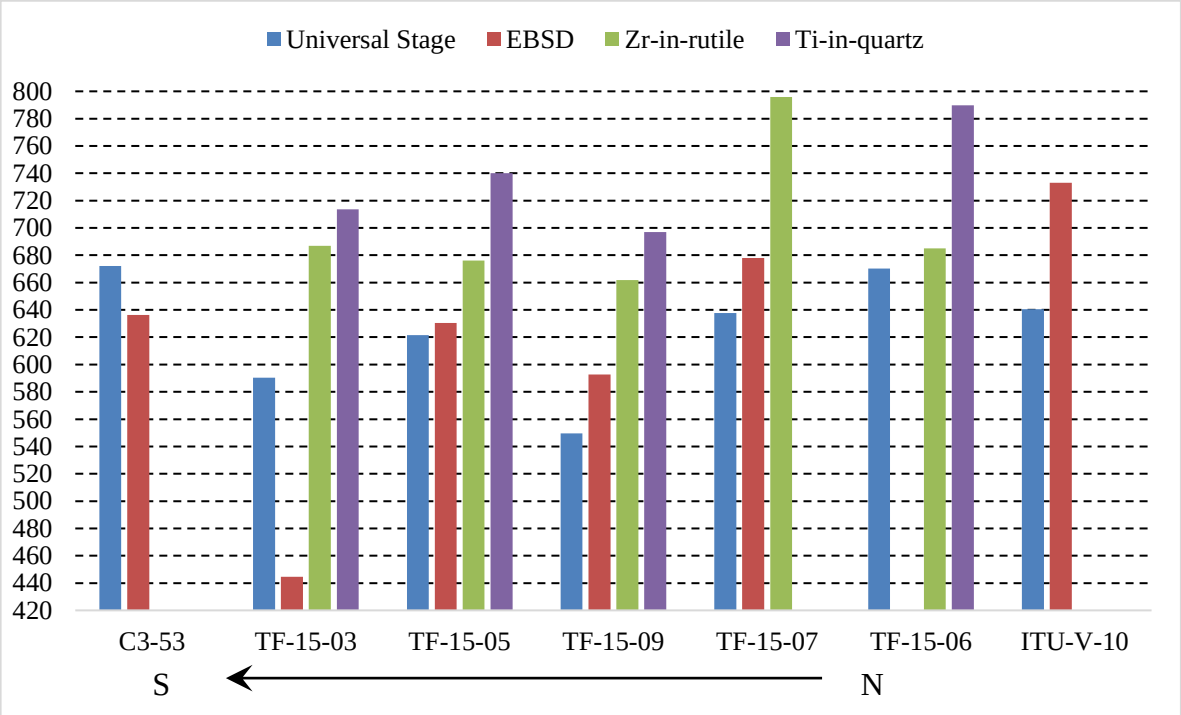

Figure 26: A comparison for all samples considering their temperatures in regarding the analysis. In blue are the results for Universal Stage; red for EBSD; green for Zr-in-rutile and, in purple, Ti-in-quartz. The metamosphism grade increases from North so South.

Plotting the samples on a metamorphic map (Figure 27) compiled from Silva (2010), it is possible to identify the mineral assemblages for each location, being chloritoid + chlorite + staurolite + garnet + muscovite + quartz for Serra da Estância and Serra do Pombeiro (A; Figure 27) and for Serra de Carrancas, the mineral assemblage is staurolite + garnet + kyanite + muscovite + quartz (B; Figure 27).

Comparing the temperatures obtained for each analysis, considering the error among each technique, except the temperatures of Ti-in-quartz, the results are in agreement with the *P-T* estimates from KFMASH (Spear, 1999). For Serra the Carrancas, temperatures are close to the expected results (Table 4).

Table 4: Temperature range for each analysis regarding each location. The thermobarometry for Serra da Estância and Serra do Pombeiro are from Pava (2010) and the temperature for Serra de Carrancas is from Garcia (2010).

	Serra da Estância	Serra do Pombeiro	Serra de Carrancas
Thermobarometry (°C)	586 ± 2	586 ± 2	641 ± 35
Universal Stage (°C)	640 - 670	550 - 640	590 - 670
EBSD (°C)	770	592 - 678	630 - 636
Zr-in-rutile (°C)	650	660 - 670	660 - 670
Ti-in-quartz (°C)	700 - 780	658 - 700	700 - 740
Zr vs. Ti (crystallization) (°C; kbar)	640; 7.0	650; 10.1	655 – 660; 9.5 – 9.7

The paragenesis for Serra da Estância and Serra do Pombeiro contemplates a *P-T* range of 5 to 13 kbar and 550 to 620 °C (A, Figure 28), and for Serra de Carrancas the *P-T* ranges from 5 to 12.5 kbar and 570 to 690 °C (B, Figure 28). Analyzing the range of temperatures of table 4 and the *P-T* range for each paragenesis, the results for Serra da Estância and Serra do Pombeiro are similar to predicted once there are the uncertainty of each analysis to be considered, which gives a good range for the results. For the temperatures of Serra de Carrancas, the results were close to the expectations, also considering the uncertainty from each analysis. The only thermometer that did not fulfill the expectations was the Ti-in-quartz.

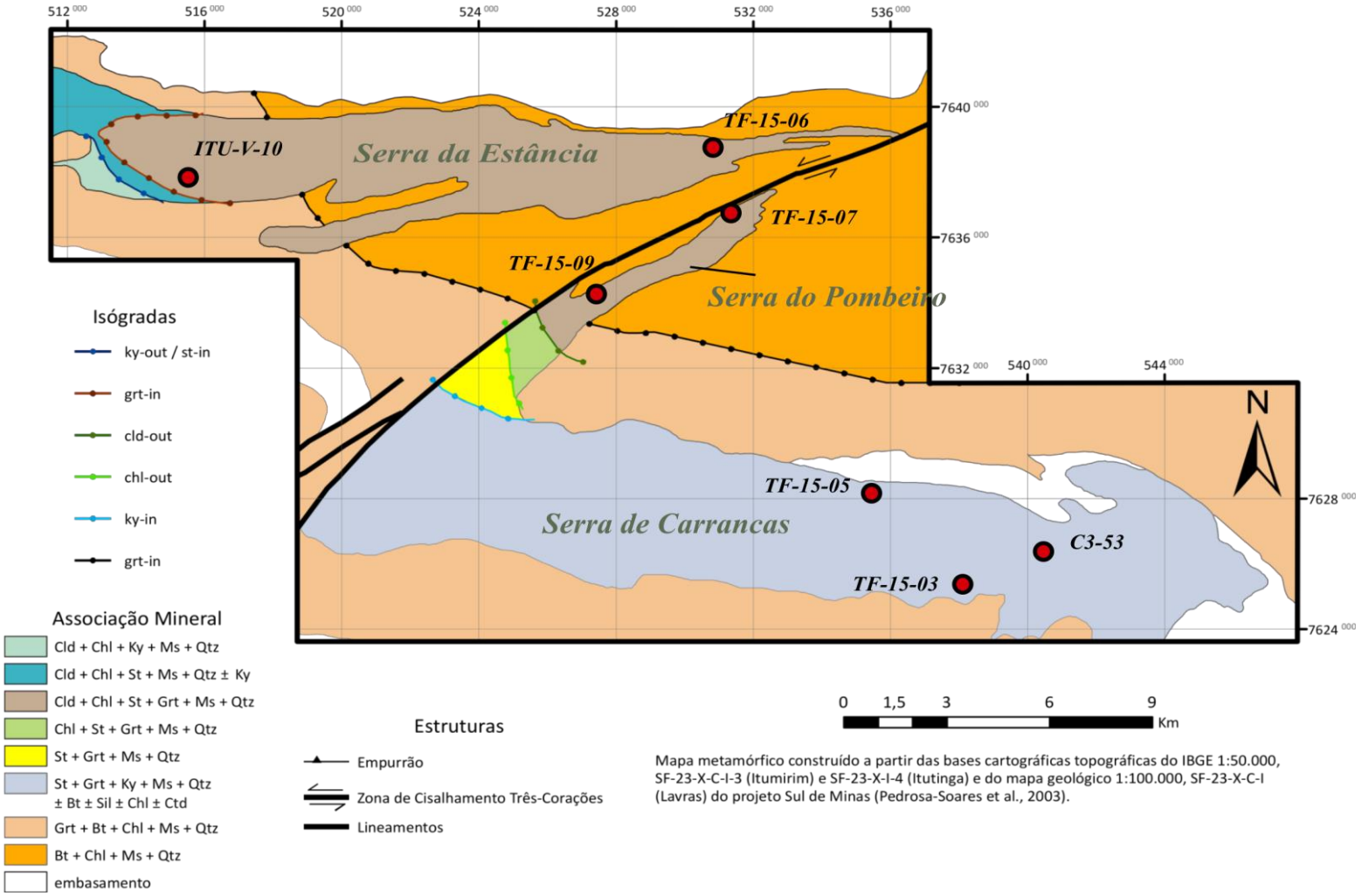

Figure 27: Metamorphic map from central Carrancas *klippe*. In red are the location of the studied samples and the location of Serra de Carrancas, Serra do Pombeiro and Serra da Estância. Modified from Silva (2010).

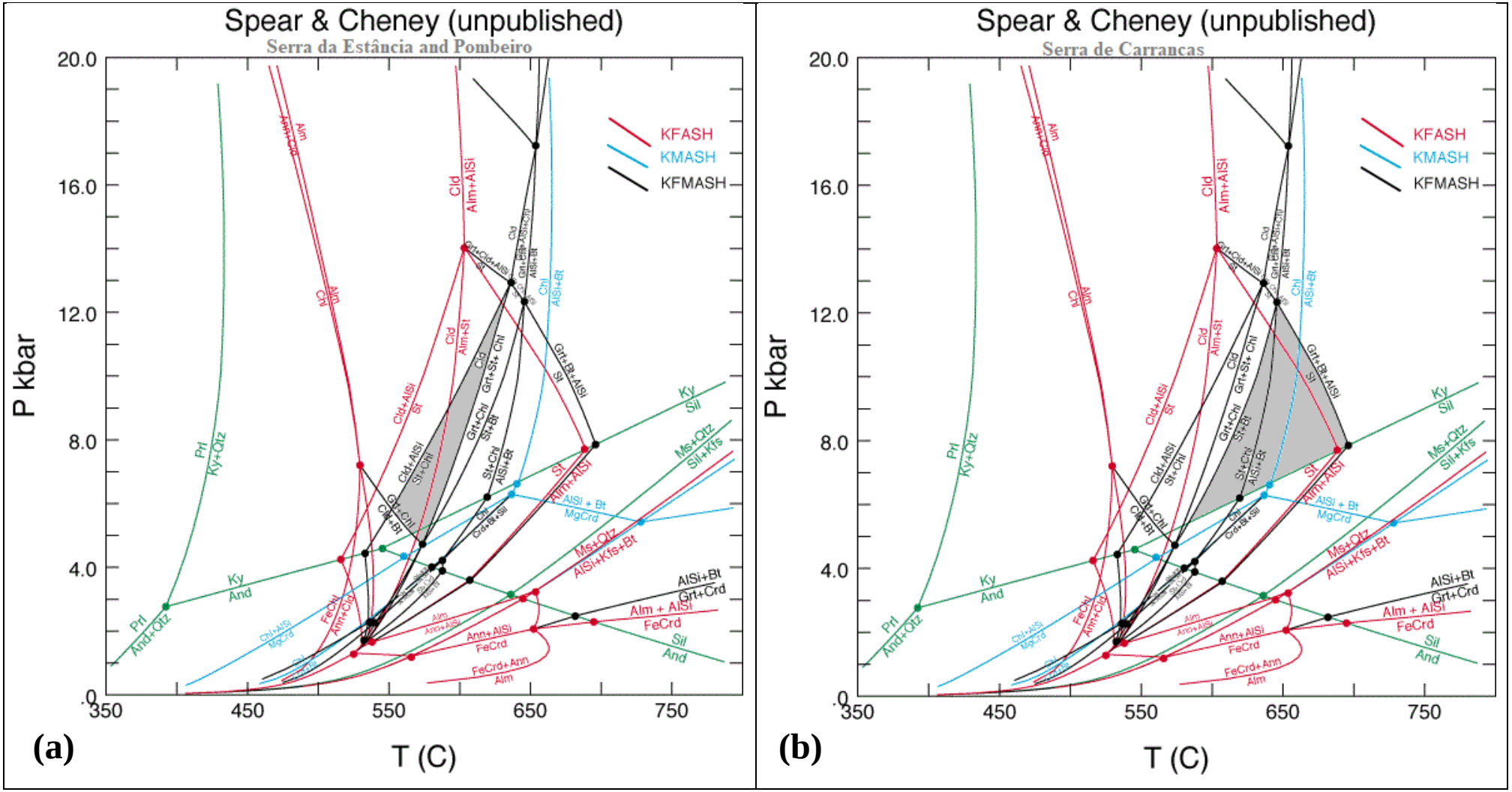

Figure 28: KFMASH grids for Serra da Estância and Serra do Pombeiro (a) and for Serra de Carrancas (b). Modified from Spear (1999).

CHAPTER 4 – CONCLUSIONS

The present work establishes the relationship of temperature of metamorphism and deformation of Carrancas Group quartzites, based on quartz c-axis thermometer calculated with Universal Stage, EBSD techniques and trace elements thermometers, therefore, to evaluate and compare the results and its metamorphic-deformation meaning.

The temperatures were obtained with the opening angle calibration of Faleiros *et al*. (2017) for the girdles generated from Hunter *et al*. (2018) script, using the open source Matlab® toolbox MTEX (Bachmann *et al*., 2010), for universal stage and EBSD. The trace elements thermometers were based on the calibrations of Tomkins *et al*. (2007) for the Zr-in-rutile analysis and Thomas *et al*. (2010) for Ti-in-quartz analysis.

The rocks from Carrancas Group were chosen because they are a well-studied for metamorphism (Ribeiro & Heilbron, 1982; Silva, 2010; Garcia, 2010), and on account of quartzite is a convenient rock for this study of quartz c-axis tilt and trace elements thermometers for understanding the metamorphic grade and deformation.

For comparison purposes *P-T* values were taken from previous studies, being 641 ± 35 °C and 11.16 ± 2,2 kbar for the Serra de Carrancas (Garcia, 2010) and 586 ± 2 °C and 10.65 kbar for the Serra do Pombeiro and Serra da Estância (Silva, 2010). Considering the work by Ashley and Law (2015) and previous *P-T* estimations, the α_{TiO_2} ~1 is adopted in this work.

The results for Serra da Estância are consistent, ranging from 640 to 670 °C for calculations made with Universal Stage measurements, 650 °C for Zr-in-rutile but, for the temperatures for EBSD and Ti-in-quartz, the temperatures were higher, 770 °C and 700 – 780 °C, respectively. However, intercepting the Zr-in-rutile and Ti-in-quartz temperatures, giving the temperature of crystallization of quartz and rutile, resulted in 640 °C and 7.0 kbar for Serra da Estância, which is too high for temperature and too low for pressure when compare to previous data based in mineral assemblage and thermobarometry.

The results for Serra do Pombeiro met the expectations, considering the results for Universal Stage, ranging from 550 to 640 °C, the Zr-in-rutile, from 660 to 670 °C and, for both EBSD and Ti-in-quartz, the temperatures are higher than the expected, being, for the first around 592 and 678 °C and around 658 and 700 °C for the last.

The results for Serra de Carrancas are in correspondence with the expected for Universal Stage analysis, ranging from 590 to 670 °C, for EBSD, ranging from 630 to 636 °C and for Zr-in-rutile, ranging from 660 to 670 °C, but, for Ti-in-quartz temperatures, the results are in disparity, ranging from 700 to 740 °C.

Taking into account these results, it is interesting to note that the Universal Stage produced a temperature result that fits very well with metamorphic peak previously calculated, and it seems to be a very reliable, cheap and relatively fast method.

The stereograms made with EBSD data produced blurred girdles. It is not clear if the acquired data was either made properly or if this is a result of superimposed events of deformations, as suggested by petrography.

The trace elements thermometers, together, give an important temperature of a simultaneous crystallization of quartz and rutile (Thomas *et al*., 2010), and partially agree with the thermobarometry results of the literature, but only for the samples TF-15-03 and TF-15-05, located at Serra de Carrancas, ranging the temperatures around 655 to 660 °C and pressure around 9.5 and 9.7 kbar. The Zr-in-rutile, alone, is a good thermometer for the Serra de Carrancas samples, with the temperature of 641 °C (Garcia, 2010), but the same cannot be applied for the samples of Serra da Estância and Serra do Pombeiro, with temperature of 586 °C (Silva, 2010), because according to studies of Cruz-Uribe *et al*. (2018), at temperatures below 600 °C, it does not activate the zircon to participate on cation exchange with other minerals, so the Zr concentration on rutile is considered to be from the source rock, and not related to deformation or metamorphism.

The Ti-in-quartz was not a reliable thermometer for this case study. The temperatures are higher than the expected and the hypothesis is that the quartz grains might not have enough energy to exchange cations with rutile and zircon during the deformation and metamorphism caused by shear zones on Carrancas *klippe*. For further investigation, it is interesting to use cathodoluminescence that might map the Ti concentration zones on quartz grains to identify portions with different Ti concentrations and investigate their relationship with possible recrystallization textures.

The intention of this work was to compare the different thermometers and to correlate their results to previous results from the literature (Silva, 2010; Garcia, 2010). The c-axis fabric open angle thermometer with measurements obtained with Universal Stage is a very good and efficient technique and seems to be more efficient and clear

than EBSD, even if this conclusion might be controversial. The first yielded temperatures compared to what Silva (2010) and Garcia (2010) calculated and within of the limits of stability field of mineral assemblages.

REFERENCES

Ashley, K. T., Carlson, W. D., Law, R. D., & Tracy, R. J. (2014).Ti resetting in quartz during dynamic recrystallization: Mechanisms and significance. American Mineralogist, 99 (10), 2025-2030.

Ashley, K. T., & Law, R. D. (2015). Modeling prograde TiO 2 activity and its significance for Ti-in-quartz thermobarometry of pelitic metamorphic rocks. Contributions to Mineralogy and Petrology, 169(2), 23.

Bachmann, F., Hielscher, R., & Schaeben, H. (2010). Texture analysis with MTEX–free and open source software toolbox. In Solid State Phenomena (Vol. 160, pp. 63-68). Trans Tech Publications.

Campos Neto, M. C., & Caby, R. (2000).Terrane accretion and upward extrusion of high-pressure granulites in the Neoproterozoic nappes of southeast Brazil: Petrologic and structural constraints. Tectonics, 19(4), 669-687.

Campos Neto, M.C., Basei, M.A.S., Vlach, S.R.F., Caby, R., Szabó, G.A.J. &Vasconcelos, P., (2004). Migração de orógenos e superposição de orogêneses; um esboço da colagem Brasiliana no sul do cráton São Francisco, SE, Brasil. *Geologia USP: Série Científica*, 4(1), 13-40.

Campos Neto, M.C., Basei, M.A.S., Janasi, V.A., Moraes, R. 2011. Orogen migration and tectonic setting of the Andrelândia Nappe system: An Ediacaran western Gondwana collage, south of São Francisco craton. Journalof South American Earth Sciences, 39: 393-406.

Cherniak, D. J., Watson, E. B., & Wark, D. A. (2007). Ti diffusion in quartz. Chemical Geology, 236(1-2), 65-74.

Coutinho, L. (2012). Estrutura, litoestratigrafia e metamorfismo do Grupo Carrancas na frente orogênica da Faixa Brasília Meridional. Dissertação (Mestrado). São Paulo: Instituto de Geociências USP.

Cruz-Uribe, A. M., Feineman, M. D., Zack, T., & Jacob, D. E. (2018). Assessing trace element (dis) equilibrium and the application of single element thermometers in metamorphic rocks. Lithos, 314-315, 1-15.

Derez, T., Pennock, G., Drury, M., Sintubin, M. (2015). Low - temperature intracrystalline deformation microstructures in quartz. Journal of Structural Geology, 71, 3-23.

Dingley, D. J., Baba-Kishi, K. Z., Randle, V. (1995). Atlas of Backscattering Kikuchi

Diffraction Patterns. *Institute of Physics Publishing*, Bristol and Philadelphia. 135 p.

Ebert, H. (1968). Ocorrências de fácies granulíticas no sul de Minas Gerais e em áreas adjacentes em dependência da estrutura orogênica: hipóteses sobre sua origem. An. Acad. Bras. Ciênc, 40 (Suplemento).

Ebert, H., & SBG. (1971). Os Paraibides entre São João del Rei, Minas Gerais, e Itapira, São Paulo, e a bifurcação entre Paraibides e Araxaides. SBG, Congr Bras Geol, 37, 177-188.

Faleiros, F. M., Moraes, R., Silva, M., & Campanha, G. A. C. (2016). A new empirical calibration of the quartz c-axis fabric opening-angle deformation thermometer. Tectonophysics, 671, 173-182.

Fazio, E., Punturo, R., Cirrincione, R., Kern, H., Pezzino, A., Wenk, H. R., ... & Mamtani, M. A. (2017). Quartz preferred orientation in naturally deformed mylonitic rocks (Montalto shear zone–Italy): a comparison of results by different techniques, their advantages and limitations. International Journal of Earth Sciences, 106(7), 2259-2278.

Garcia, L. L. S. (2010). *Mapa Metamórfico das Rochas do Grupo Carrancas na Região das Serras de Carracas, Bicas e Moleque, Sul de Minas Gerais*. Monografia de Trabalho de Formatura. São Paulo: Instituto de Geociências USP.

Gleason, G.C., Tullis, J., Heidelbach, F., (1993). The role of dynamic recrystallization in the development of lattice preferred orientations in experimentally deformed quartz aggregates. Journal of Structural Geology, 15, 1145-1168.

Goldstein, J. I., Newbury, D. E., Michael, J. R., Ritchie, N. W., Scott, J. H. J., & Joy, D. C. (2007). Scanning electron microscopy and X-ray microanalysis. Springer.

Heilbron, M. (1983). Dados preliminaressobre a geologia e o metamorfismo da área entre Itutinga e Madre de Deus (MG). Simpósio de Geologia de Minas Gerais, 2, Belo Horizonte, Anais, SBG-MG, vol.3, 387-401.

Hunter, N. J. R., Weinberg, R. F., Wilson, C. J. L., & Law, R. D. (2018). A new technique for quantifying symmetry and opening angles in quartz c-axis pole figures: Implications for interpreting the kinematic and thermal properties of rocks. Journal of Structural Geology, 112, 1-6.

Kruhl, J.H. (1986). Textures and c-axis orientations of deformed quartz crystals from porphyric dikes of the Alpine Root Zone. (Western Alps). *Geologische Rundschau*, 75(3), 601-623.

Kruhl, J.H. (1996). Prism- and basal-plane parallel subgrain boundaries in quartz: a

microstructural geothermobarometer. *Journal of Metamorphic Geology*, 14, 581–589.

Kruhl, J.H., Nega, M., (1996). The fractal shape of sutured quartz grain boundaries: application as a geothermometer. *Geologische Rundschau*, 85, 38-43.

Law, R.D. (2014). Deformation thermometry based on quartz c-axis fabrics and recrystallization microstructures: A review. *Journal of Structural Geology*, 66, 129-161.

Morales, L. F. G., Hinrichs, R., & Fernandes, L. A. D. Á. (2007). A técnica de difração de elétrons retro-espalhados (EBSD) em microscópio eletrônico de varredura (MEV) e sua aplicação no estudo de rochas deformadas. *Pesquisas em Geociências*. Vol. 34, n. 1 (jan./jun. 2007), p. 19-34.

Paciullo, F. P., Fonseca, A. C., Andreis, R. R., Ribeiro, A., Trouw, R. A., & Wiedemann, C. M. (1996). Contribuição à geologia do sul de Minas Gerais edição das folhas 1: 50.000 Itumirim, Itutinga, Madre de Deus, Luminárias, Minduri e Andrelândia. Anuário do Instituto de Geociências, 19, 123-142.

Paciullo, F. V., Ribeiro, A., & Trouw, R. A. (2003). Geologia da Folha Andrelândia 1: 100.000. Geologia e recursos minerais do sudeste mineiro. Projeto Sul de Minas-Etapa I, 84-119.

Paciullo, F. V. P., Ribeiro, A., Andreis, R. R., & Trouw, R. A. J. (2017). The Andrelândia basin, a Neoproterozoic intraplate continental margin, southern Brasília Belt, Brazil. Revista Brasileira de Geociências, 30(1), 200-202.

Passchier, C.W., Trouw, R.A.J., Zwart, H.J. & Vissers, R.L.M. 1992. Porphyroblast rotation: eppur si muove? Journal Metamorphic Geology.10: 283 - 294.

Passchier, C.W., Trouw, R.A.J. (2005). *Microtectonics*.2nd Ed. Springer Verlag, New York, Berlin, 289 pp.

Powell, R., Holland, T.J.B. (1990). Calculated mineral equilibria in thepelite system, KFMASH (K2O - FeO - MgO - Al2O3 - SiO2 - H2O). *American Mineralogist* 75, 367 - 380.

Prior, D. J., Boyle, A. P., Brenker, F., Cheadle, M. C., Day, A., Lopez, G., Peruzzo, L., Potts, G. J., Reddy, S., Spiess, R., Timms, N. E., Trimby, P., Wheeler, J. & Zetterstrom, L. (1999). The application of electron backscatter diffraction and orientation contrast imaging in the SEM to textural problems in rocks. *American Mineralogist*, 84 (11-12), 1741-1759.

Randle, V. (2000). Theoretical framework for electron backscatter diffraction. In

Electron Backscatter Diffraction in Materials Science (pp. 19-30). *Springer*, Boston, MA.

Randle, V., & Engler, O. (2000). Introduction to Texture Analysis: Macrotexture, Microtexture and Orientation Mapping. Gordon & Breach Science Publishers. Reading, UK.

Ribeiro, A., Heilbron, M. (1982). Estratigrafia e Metamorfismo dos Grupos Carrancas e Andrelândia, sul de Minas Gerais. *Anais da Academia Brasileira de Ciências*, 32(1), 177-186.

Ribeiro, A. Trouw, R.A. J., Andreis, R. R., Paciullo, F. V. P., Valença, J. (1995). Evolução das bacias Proterozóicas e o termotectonismo-brasiliano na margem sul do cráton São Francisco. *Revista Brasileira de Geociências*, v.25, 235-248.

Silva, M. P. (2010). Modelamento metamórfico de rochas das fácies xisto-verde e Anfibolito com o uso de pseudosseções: exemplo das rochas da Klippe Carrancas, sul de Minas Gerais. Dissertação (Mestrado). São Paulo: Instituto de Geociências USP.

Spear, F.S., Cheney, J.T. (1989). A petrogenetic grid for pelitesschsts in the system SiO2 - Al2O3 - FeO - MgO - K2O - H2O.*Contribution to Mineralogy and Petrology* 101, 149 - 164.

Spear, F.S. (1989). Petrologic Determination of metamorphic pressure-temperature-time paths. In: Spear, F. & Peacock, S. M (1989). Metamorphic Pressure-Temperature-Time Paths. Short Course in Geology. vol. 7. 28th International Geology Congress. Washington, DC. 1 -55.

Spear, F. S. (1999). Real-time AFM diagrams on your Macintosh. Geological Materials Research, 1(3), 1-18.

Stipp, M., Stuènitz, H., Heilbronner, R., &Schmid, S. M. (2002). The eastern Tonale fault zone: a 'natural laboratory' for crystal plastic deformation of quartz over a temperature range from 250 to 700 C. *Journal of Structural Geology*, 24(12), 1861-1884.

Thomas, J.B., Watson, E.B., Spear, F.S., Shemella, P.T., Nayak. S.J., Lanzirotti. A. (2010). TitaniQ under pressure: the effect of pressure and temperature on the solubility of Ti in quartz. *Contributions to Mineralogy and Petrology*, 160: 743–759.

Tomkins, H. S., Powell, R. Ellis, D.J. (2007). The pressure dependence of the zirconium-in-rutile thermometer. *Journal of Metamorphic Geology*, 25(6), 703-713.

Trouw, R.A.J., Ribeiro, A., Paciullo, F.V.P. (1983). Geologia estrutural dos Grupos São João Del Rei, Carrancas e Andrelândia, sul de Minas Gerais. *Anais da Academia Brasileira de Ciências*, 55(1), 71-85.

Wahlstrom, E.E. (1969). Cristalografia Óptica. São Paulo: Ao Livro Técnico.

Wark D.A., Watson E.B. (2006). TitaniQ: a titanium-in-quartz geothermometer. *Contributions to Mineralogy and Petrology*, 152, 743–754.

Watson, E.B., Wark, D.A., Thomas, J.B. (2006). Crystallization thermometers for zircon and rutile. *Contributions to Mineralogy and Petrology*, 151, 413-433.

Wahlstrom, E.E. (1969). *Cristalografia Óptica*. São Paulo: Ao Livro Técnico.

Westin, A., & Neto, M. D. C. C. (2013). Provenance and tectonic setting of the external nappe of the Southern Brasília Orogen. *Journal of South American Earth Sciences*, *48*, 220-239.

Westin, A. (2015). Depósitos Orogênicos e Bacia Extencional: o Embasamento Metassedimentar e a Cobertura da Margem Passiva no Orógeno Brasília Meridional (Doutorado). São Paulo: Instituto de Geociências USP.

Westin, A., Neto, M. C. C., Hawkesworth, C. J., Cawood, P. A., Dhuime, B., & Delavault, H. (2016). A paleoproterozoic intra-arc basin associated with a juvenile source in the Southern Brasilia Orogen: Application of U–Pb and Hf–Nd isotopic analyses to provenance studies of complex areas. *Precambrian Research*, *276*, 178-193.

White, S. (1977). Geological significance of recovery and recrystallization processes in quartz. *Tectonophysics*, 39, 143-170.

Zwart, H.J. 1962. On the determination of polymetamorphic mineral associations and its application to the Bosost area (Central Pyrenees). Geologische Rundschau, 52, 38–65.